

Identification algorithms for time-dependent materials

Citation for published version (APA):

Op den Camp, O. M. G. C. (1996). *Identification algorithms for time-dependent materials*. [Phd Thesis 1 (Research TU/e / Graduation TU/e), Mechanical Engineering]. Technische Universiteit Eindhoven.
<https://doi.org/10.6100/IR459234>

DOI:

[10.6100/IR459234](https://doi.org/10.6100/IR459234)

Document status and date:

Published: 01/01/1996

Document Version:

Publisher's PDF, also known as Version of Record (includes final page, issue and volume numbers)

Please check the document version of this publication:

- A submitted manuscript is the version of the article upon submission and before peer-review. There can be important differences between the submitted version and the official published version of record. People interested in the research are advised to contact the author for the final version of the publication, or visit the DOI to the publisher's website.
- The final author version and the galley proof are versions of the publication after peer review.
- The final published version features the final layout of the paper including the volume, issue and page numbers.

[Link to publication](#)

General rights

Copyright and moral rights for the publications made accessible in the public portal are retained by the authors and/or other copyright owners and it is a condition of accessing publications that users recognise and abide by the legal requirements associated with these rights.

- Users may download and print one copy of any publication from the public portal for the purpose of private study or research.
- You may not further distribute the material or use it for any profit-making activity or commercial gain
- You may freely distribute the URL identifying the publication in the public portal.

If the publication is distributed under the terms of Article 25fa of the Dutch Copyright Act, indicated by the "Taverne" license above, please follow below link for the End User Agreement:

www.tue.nl/taverne

Take down policy

If you believe that this document breaches copyright please contact us at:

openaccess@tue.nl

providing details and we will investigate your claim.



Olaf Op den Camp

Identification Algorithms for Time-Dependent Materials

Identification Algorithms
for
Time-Dependent Materials

CIP-DATA KONINKLIJKE BIBLIOTHEEK, DEN HAAG

Camp, Olaf Martinus Gerardus Christiaan Op den

Identification algorithms for time-dependent materials /
Olaf Martinus Gerardus Christiaan Op den Camp.- [S.l. :s.n.]
Thesis Technische Universiteit Eindhoven.- With ref.
ISBN 90-386-0427-0

Subject headings: identification algorithms / material
characterization / fluid-solid mixtures.

Druk: Krips Repro Meppel

Identification Algorithms for Time-Dependent Materials

Proefschrift

ter verkrijging van de graad van doctor
aan de Technische Universiteit Eindhoven,
op gezag van de Rector Magnificus, prof.dr. J.H. van Lint,
voor een commissie aangewezen door het College van Dekanen,
in het openbaar te verdedigen
op woensdag 8 mei 1996 om 16.00 uur

door

Olaf Martinus Gerardus Christiaan Op den Camp

geboren te Swalmen

Dit proefschrift is goedgekeurd door de promotoren:

prof.dr.ir. J.D. Janssen

prof.dr.ir. J.J. Kok

en de copromotor:

dr.ir. C.W.J. Oomens

Contents

Summary	5
Notation	7
1 Introduction	9
2 Analysis of fluid-solid mixtures	17
2.1 Introduction	17
2.2 Formulation of the model equations	17
2.3 Solving the model equations	23
2.3.1 Spatial discretisation	23
2.3.2 Determination of the nodal quantities	24
2.3.3 Parameter variations	26
2.3.4 Concluding remarks	26
2.4 The output equation and the sensitivity matrix	27
2.4.1 The output equation	27
2.4.2 The sensitivity matrix	27
3 A recursive estimation algorithm	29
3.1 Introduction	29
3.2 The determination of parameters	30
3.2.1 The method of least squares	30
3.2.2 The recursive approach	30
3.3 The recursive estimation algorithm	32
3.3.1 Solving the minimisation problem	32
3.3.2 Specification of the weighting matrices	33
3.4 Testing of the recursive algorithm	34
3.4.1 Constitutive behaviour	35

3.4.2	'Experimental' set-up	36
3.4.3	Finite element analysis	37
3.4.4	Parameter estimation	40
3.4.5	Influence of a model error	41
3.5	Discussion	44
4	An estimation algorithm with residuals on the model equations	47
4.1	Introduction	47
4.2	The integral estimation algorithm	48
4.3	Solving the boundary value problem	50
4.4	Testing of the integral algorithm	52
4.4.1	'Experimental' set-up	52
4.4.2	Finite element analysis	54
4.4.3	Parameter estimation	54
4.4.4	Influence of a model error	57
4.5	Discussion	59
5	Discussion, conclusions and recommendations	61
5.1	Discussion	61
5.2	Conclusions	64
5.3	Recommendations	65
	Bibliography	67
A	Finite element formulation of the model equations	71
B	Scheme of the recursive algorithm	79
C	Formulation of the boundary value problem	81
D	The transformation matrix in the approximating linearisation method	83
	Curriculum Vitae	85
	Dankwoord	87
	Samenvatting	89

Summary

With standard methods for the determination of material parameters, the loading conditions and the geometry of specimen are generally chosen such that measured boundary loads and displacements can easily be translated to local stresses and strains, which are subsequently used to determine the parameters in a material model. If the material is inhomogeneous, or if manufacturing of specimen is difficult or undesirable, then these methods are unsuitable and the numerical-experimental technique may be used. This technique uses of experiments where as much field information (displacement fields, pressures, velocities) as possible is measured in stead of boundary information only. By confronting this information with (numerical) calculations on the basis of an assumed material model and initial guesses for the material parameters, the parameters are iteratively adapted via an estimation algorithm until convergence is achieved. This method offers much more freedom than standard experimental methods, but until now it was particularly applied to materials showing time-*independent* behaviour.

The objective of this thesis was to study several algorithms that can be applied to materials showing time-dependent behaviour. A fully recursive and an integral estimation algorithm have been implemented and investigated. The algorithms have been applied to mixture materials consisting of a porous solid, saturated by a fluid. The interaction between solid and fluid leads to viscoelastic behaviour.

The differential and algebraic model equations, describing this behaviour, are nonlinear in the displacements and the parameters and linear in the pressures. The used field information consists of displacements and pressures. The algorithms have been tested by means of simulations. The results of an analysis with an assumed material model and chosen parameters, are disturbed by noise to represent observations out of an experiment. Subsequently, the estimation model is initialised with different values of the material parameters. The difference between the 'experimental' results and the results of analyses with the model is used to determine the material parameters by means of the estimation algorithm. The estimation process is considered to be verified if these parameters converge on the values used to generate the 'observations'. Analyses with and without model errors have been performed.

The most important conclusion is that both algorithms can be used to determine the material parameters for this type of material. The recursive algorithm is extremely efficient. The time required to estimate the material parameters is of the same order as the time required for a single analysis with given parameters. The integral algorithm is very time-consuming and leads to a difficult two-point-boundary-value problem. At the moment no generally applicable and satisfying solution strategy to this problem has been found.

Notation

a	scalar	
\underline{a}	column of scalars	$(\underline{a})_i = a_i$
\underline{A}	matrix of scalars	$(\underline{A})_{ij} = A_{ij}$
\underline{A}^T	transpose of matrix	$(\underline{A}^T)_{ij} = A_{ji}$
\underline{A}^{-1}	inverse of matrix	$\underline{A} \underline{A}^{-1} = \underline{I}$
\underline{I}	unit matrix	$\underline{A} \underline{I} = \underline{A}$
\vec{a}	vector	
$\vec{\underline{a}}$	column of vectors	$(\vec{\underline{a}})_i = \vec{a}_i$
$\vec{\underline{A}}$	matrix of vectors	$(\vec{\underline{A}})_{ij} = \vec{A}_{ij}$
\mathbf{A}	second order tensor	
\mathbf{A}^c	conjugate of tensor	
\mathbf{A}^{-1}	inverse of tensor	$\mathbf{A} \cdot \mathbf{A}^{-1} = \mathbf{I}$
\mathbf{I}	unit tensor	$\mathbf{A} \cdot \mathbf{I} = \mathbf{A}$
\hat{a}	estimate of a	
\bar{a}	true value of a	
\dot{a}	total time derivative of a	
$\partial a / \partial t$	spatial time derivative of a	

Chapter 1

Introduction

The research presented in this thesis concerns the development of algorithms to estimate parameters in the constitutive models for time-dependent materials. Starting point has been the numerical-experimental method as developed by Hendriks [1991]. In this chapter firstly this method will be described. Then, some of its accomplishments and shortcomings will be given. This will supply arguments to put effort in the development of estimation algorithms for time-dependent materials. The research is focused on two-component fluid-solid mixture models, i.e. a subclass of the models used to describe time-dependent material behaviour. Many of the ideas put forward in this thesis can be generalised to other classes. The chapter will finish with a brief outline of the thesis.

The introduction of the numerical-experimental technique was initiated by difficulties with the characterisation of complex materials, in particular soft biological tissues, which show inhomogeneous, anisotropic, time-dependent, and both physically and geometrically nonlinear behaviour (Hendriks [1991], Oomens *et al.* [1993]). To distinguish these phenomena, experiments on specimens have to yield sufficient information. With standard experiments for the characterisation of materials, in particular global and boundary information, such as measured forces and boundary displacements, is used. For example, in solid mechanics the geometry of the specimen is often chosen such that in a substantial part of the specimen a homogeneous stress and strain field is present. Then, in that part of the specimen the stress and strain can be derived from the force and displacement measured on the boundary. The result is used to determine the model parameters.

The numerical-experimental technique makes use of experiments where as much field information as possible is measured, instead of boundary information only. Measured quantities may be displacements, velocities, strains, forces, pressures, or stresses. A constitutive model, which is

already pointed out that modelling of boundary conditions can be rather difficult, e.g. due to slip in clamps. In that case the relation between the input and the boundary conditions is not straightforward.

The numerical-experimental technique has major advantages compared to standard material identification methods, since it can handle inhomogeneous stress and strain fields. It is no longer necessary to manufacture specimens and to apply loads in such a way that a homogeneous stress and strain field is realised in a well-defined region of the specimen. Experiments can be designed for specimens with rather arbitrary geometry, and cutting specimens of a specific prescribed geometry is no longer required. Even testing in-situ becomes possible. The latter is especially important for materials with long fibres, such as soft biological tissues, because the internal structure of the material can be maintained and there is no loss of interaction between different material directions. Moreover, application of the numerical-experimental technique may lead to an accurate estimation of the model parameters, as much information becomes available from measurements.

Hendriks [1991] successfully applied the numerical-experimental technique in an experiment with a synthetic membrane. The material was modeled as an orthotropic linear elastic membrane with local axes of symmetry varying with the position in the material. Breukink [1994] and van Ratingen *et al.* [1993] used this technique to determine the mechanical properties of human skin in-vivo and canine skin in-vitro respectively, using the same elastic model.

Many complex materials, such as soft biological tissues, polymer melts and solutions, or thermoplastics, show time-dependent behaviour. Then, the current stress in the material not only depends on the current strain but on the entire strain history and purely elastic models are unsuitable.

Originally, the numerical-experimental technique according to Hendriks was developed to be universally applicable to any type of material, including time-dependent materials. For the analyses of the experiment, the estimation algorithm was coupled to a finite element code. For each of the material models included in the code, the numerical-experimental technique should be applicable and the estimation algorithm should be able to determine the model parameters from the measured and computed field quantities.

However, previous research (Hendriks [1991], van Ratingen [1994]) has brought up several issues which have to be investigated before the numerical-experimental technique is applied to time-dependent materials:

- For the identification, field quantities are measured at subsequent points of time for a

given load history. Per point of time, the parameters are determined such that the residuals between measured and computed quantities are minimised. This requires the solution of a set of nonlinear algebraic equations in the model parameters. Therefore, a Newton-Raphson iterative procedure is used. As will be shown in Chapter 3, this leads to a set of linear equations in which two distinct parameter estimates show up: the estimate based on all measurements up to and including the previous time point and the estimate resulting from the last iteration at the current time point taking the most recent measurements into account. The algorithm according to Hendriks [1991] however did not distinguish between these estimates (van Ratingen [1994]).

- The algorithm according to Hendriks is rather inefficient. For each step in the estimation of the parameters, the numerical analysis using the updated parameter values is repeated over the total time interval up to the current point of time instead of over the last time step only. Furthermore, the sensitivity matrix is determined numerically. For these reasons, the identification of complex materials is often very laborious.
- The experiments have to provide as much information as possible on the material behaviour. One of the challenging aspects of the numerical-experimental technique is the opportunity to use this information to improve on model errors, especially errors in the constitutive model.

For the moment, the idea of one estimation algorithm for all material models in the finite element code is abandoned. Instead, algorithms for a specific class of material models are developed. Per class, the algorithms have to meet particular requirements. The research in this thesis focuses on adapting the numerical-experimental technique for the study of time-dependent materials.

To describe time-dependent behaviour, many constitutive models, varying from phenomenological models to detailed micro-structural models, can be used. This research focuses on two-component fluid-solid mixture models (Bowen [1976, 1980], Oomens *et al.* [1987], Huyghe *et al.* [1992]). A mixture consists of a solid matrix with interconnected pores, saturated with fluid. Due to mechanical loading, the interstitial fluid is forced to move through the matrix and across the mixture's surface. The interaction between the components induces a flow resistance, which depends on the permeability of the mixture and on the velocity of the fluid relative to the solid. Therefore, the stress in the material is not only a function of the solid deformation but also of the velocity of the fluid and the solid. This results in time-dependent behaviour.

There are several arguments to focus on mixture models:

- Mixture models have successfully been used in biomechanics to describe biological tissues such as articular cartilage and the meniscus (Mow *et al.* [1980], Lai and Mow

[1980], Spilker *et al.* [1988]), skin and subcutis (Oomens *et al.* [1987]), myocardial tissue (Huyghe *et al.* [1992], Bovendeerd *et al.* [1992]), and the intervertebral disk (Snijders [1994], Simon *et al.* [1985]).

- The model equations for two-component fluid-solid mixtures can easily be written in a state-space formulation which allows the use of estimation techniques originating from system and control technology.

In this thesis, a mixture of an elastic solid and an ideal fluid is considered. Aspects like aging, adaptation (for biological materials) and damage are not included. Therefore, the a priori unknown model parameters are considered to be constant, so

$$\dot{\theta} = 0, \quad (1.2)$$

where $\dot{\theta}$ is the time derivative of θ . In continuum mechanics, the parameter equation (1.2) is considered trivial and is rarely used. When parameter identification is concerned, the parameter equation is explicitly given to denote that estimation is aimed at finding constant model parameters. However, during estimation this requirement can be slightly released by allowing a small residual on $\dot{\theta}$. Then, this residual and the residual on the measurement equation (1.1) are minimised simultaneously. In this way the identification algorithm is given the opportunity to determine parameters as a function of time. Significant time-dependent behaviour of the parameter estimates may be an indication for the presence of model errors.

The objective of the present research is to develop identification algorithms for a two-component fluid-solid mixture model. In particular two issues are studied, i.e., efficiency of the algorithm and the ability to detect errors in the constitutive model by use of the algorithm. For this purpose no real experiments, but simulations of some relevant tests are performed.

Chapter 2 concerns the analysis of an ‘experiment’ on a specimen of mixture material. Given a set of parameters and the model input, the analysis has to provide the model output and the sensitivity matrix (see Figure 1.1). Therefore the model equations for a fluid-solid mixture are derived and a solution strategy is presented. If the solution to the model equations is known, the output can be determined. Furthermore, a pseudo-analytical method to determine the sensitivity matrix, is introduced.

In Chapter 3 and 4, estimation algorithms are discussed. Chapter 3 deals with a *recursive estimation algorithm*. Measurements at subsequent time points are sequentially used by the algorithm. This is shown to contribute to efficiency. A scalar measure of the residual on the parameter

equation and the difference between the measurements and the computed output is defined at each time point where measurements become available. The parameters at that time point are determined by minimising this measure with respect to the parameters, assuming that the model equations are satisfied exactly. This requires the solution of a set of algebraic equations in the model parameters. In combination with the pseudo-analytical method to determine the sensitivity matrix, a highly efficient identification technique results.

Chapter 4 presents an *integral estimation algorithm*, which uses all measurements of the total experiment simultaneously. It is not assumed that the model equations will be satisfied exactly. To account for model errors, residuals are accepted on both the model equations and the parameter equation. Therefore, straightforward solution of the model equations as discussed in Chapter 2, is not possible. Consequently, analysis and estimation are combined and a strict distinction between these two components of the numerical-experimental technique can no longer be made. After all measurements are available from an experiment, a scalar measure of the residuals on the model equations, on the parameter equation (1.2) and on the measurement equation (1.1) is set up once. Minimisation of this measure leads to a boundary value problem that is at the moment only solvable for a subclass of experiments. In contrast to the recursive algorithm, this method is time-consuming. However, the integral algorithm provides much information on the estimation process via the residuals after identification.

Finally, in Chapter 5 conclusions are drawn and some recommendations for future research are given.

Chapter 2

Analysis of fluid-solid mixtures

2.1 Introduction

Fluid-solid mixture models are used as an example to study the characterisation of time-dependent materials. The objective of this chapter is to determine the output and the sensitivity matrix for a fluid-solid mixture, given a set of parameters and the input as a function of time.

Starting from the conservation laws and the constitutive relations for the mixture components, the model equations for the total mixture are derived in Section 2.2.

A numerical method has to be used to solve the resulting set of first order partial differential equations in the solid displacement and the fluid pressure. In Section 2.3 the equations are spatially discretised by means of the finite element method and a time discretisation scheme is applied. An iterative procedure to solve the resulting nonlinear discretised model equations is elaborated. The solution strategy is discussed in detail, since the finite element method and the iterative procedure provide intermediate results which are required to determine the sensitivity matrix in an efficient way.

Section 2.4 focusses on the model output and the sensitivity matrix. The determination of the output is generally straightforward if the solution for the displacement and the pressure is known in every point of the specimen. For the efficient determination of the sensitivity matrix a pseudo-analytical technique is discussed.

2.2 Formulation of the model equations

A mixture of a solid with interconnected pores, saturated with fluid, is considered. This mixture is seen as a superposition of two continua, each occupying the total mixture volume. The

behaviour of the mixture is the result of the behaviour of the distinct components and the interaction between the components.

All properties are averaged over an elementary volume. The dimensions of this volume are chosen sufficiently large to allow a continuum representation of all discontinuous properties, and sufficiently small to avoid that macroscopic variations of the properties throughout the material are smoothed out (Biot [1941], Bowen [1976], Oomens *et al.* [1987], Huyghe [1986]). The components are seen as continua. Conservation laws will be applied to each of the components.

Let $\mathcal{C}(t)$ be the current configuration. The configuration $\mathcal{C}(t_0)$ at some reference time t_0 is called the reference configuration \mathcal{C}_0 . The volume of the mixture in $\mathcal{C}(t)$ and \mathcal{C}_0 is equal to $V(t)$ and $V_0 = V(t_0)$ respectively. The position vector of a particle of component α ($\alpha = s$ for the solid and $\alpha = f$ for the fluid) in \mathcal{C}_0 , with respect to a fixed origin \mathcal{O} , is denoted \vec{x}_0^α . Each position in the mixture is occupied by a solid and a fluid particle. The current position vector \vec{x}^α of a particle of component α with reference position vector \vec{x}_0^α is given by

$$\vec{x}^\alpha = \vec{x}_0^\alpha + \vec{q}^\alpha(\vec{x}_0^\alpha, t), \quad (2.1)$$

where \vec{q}^α is the displacement vector. The velocity \vec{v}^α is the material time derivative of \vec{q}^α , i.e.

$$\vec{v}^\alpha = \dot{\vec{x}}^\alpha = \dot{\vec{q}}^\alpha. \quad (2.2)$$

The deformation of the solid from \mathcal{C}_0 to \mathcal{C} is described by the deformation tensor \mathbf{F} ,

$$\mathbf{F} = (\vec{\nabla}_0 \vec{x}^s)^c, \quad (2.3)$$

where $\vec{\nabla}_0$ is the gradient operator with respect to the reference configuration.

Let dV be an elementary mixture volume. The part of dV that is occupied by component α is denoted by dV^α and the local volume fraction n^α of this component is defined by

$$n^\alpha = \frac{dV^\alpha}{dV}. \quad (2.4)$$

The volume fraction of the fluid, n^f , is called the *porosity* of the mixture. The sum of the volume fractions of the distinct components must be equal to 1, so

$$n^s(\vec{x}, t) + n^f(\vec{x}, t) = 1. \quad (2.5)$$

Let dm^α be the mass of component α in the considered elementary volume dV . Then the true local density $\bar{\rho}^\alpha$ is equal to

$$\bar{\rho}^\alpha = \frac{dm^\alpha}{dV^\alpha}, \quad (2.6)$$

whereas the apparent local density ρ^α is defined as

$$\rho^\alpha = \frac{dm^\alpha}{dV} = n^\alpha \bar{\rho}^\alpha. \quad (2.7)$$

For the mixtures considered in this thesis, only the balance of mass and the balance of momentum are relevant. In the balance equations, inertia effects will be neglected, as only relatively slow deformation rates are considered. Furthermore, it is assumed that there is no mass exchange between the components and that body forces are negligible. With these assumptions, the *local balance law of mass* for component α reads (Bowen [1976])

$$\frac{\partial \rho^\alpha}{\partial t} + \vec{\nabla} \cdot (\rho^\alpha \vec{v}^\alpha) = 0, \quad (2.8)$$

where $\vec{\nabla} = \mathbf{F}^{-c} \cdot \vec{\nabla}_0$ is the gradient operator with respect to the current configuration. The *local balance laws of momentum and of moment of momentum* for α are (Bowen [1976])

$$\vec{\nabla} \cdot \boldsymbol{\sigma}^\alpha + \vec{\pi}^\alpha = \vec{0}, \quad (2.9)$$

$$\boldsymbol{\sigma}^\alpha = (\boldsymbol{\sigma}^\alpha)^T, \quad (2.10)$$

where $\boldsymbol{\sigma}^\alpha$ is the Cauchy stress tensor and $\vec{\pi}^\alpha$ represents the body force on α due to interaction with the other constituent. The balance of momentum for the total mixture leads to the restriction

$$\vec{\pi}^s + \vec{\pi}^f = \vec{0}. \quad (2.11)$$

From (2.9) and (2.11) it is readily seen that

$$\vec{\nabla} \cdot (\boldsymbol{\sigma}^s + \boldsymbol{\sigma}^f) = \vec{0}, \quad \vec{\nabla} \cdot \boldsymbol{\sigma}^f + \vec{\pi}^f = \vec{0}. \quad (2.12)$$

To arrive at a complete set of equations for the characterisation of the behaviour of a mixture, constitutive relations for the components and for the interaction force between the components are introduced:

- Both fluid and solid are intrinsically incompressible. This implies that the true local density $\bar{\rho}^\alpha$ for each of the components is constant, so

$$\dot{\bar{\rho}}^\alpha = 0, \quad \vec{\nabla} \bar{\rho}^\alpha = \vec{0}. \quad (2.13)$$

As a result, the local balance law of mass becomes

$$\frac{\partial n^\alpha}{\partial t} + \vec{\nabla} \cdot (n^\alpha \vec{v}^\alpha) = 0, \quad (2.14)$$

and, since $n^s + n^f = 1$, this results in

$$\vec{\nabla} \cdot (n^s \vec{v}^s + n^f \vec{v}^f) = \vec{\nabla} \cdot \vec{v}^s + \vec{\nabla} \cdot (n^f (\vec{v}^f - \vec{v}^s)) = 0. \quad (2.15)$$

Equation (2.15) can be interpreted as the balance of mass for the total mixture.

- According to Oomens *et al.* [1987], the solid stress tensor σ^s equals

$$\sigma^s = -n^s p \mathbf{I} + \tau^s. \quad (2.16)$$

Here p is the fluid pressure, \mathbf{I} is the unit tensor, and τ^s is the effective Cauchy stress tensor. The term $-n^s p \mathbf{I}$ results from the intrinsic incompressibility of the solid.

The proposed elastic constitutive model for the solid, that satisfies objectivity (Hunter [1983]), is given by

$$\tau^s = \frac{1}{J} \mathbf{F} \cdot \mathbf{S}(\mathbf{C}, \vartheta) \cdot \mathbf{F}^c, \quad (2.17)$$

where $J = \det(\mathbf{F})$ is the volume ratio of current state and reference state and \mathbf{S} is a tensor function of the Cauchy-Green tensor $\mathbf{C} = \mathbf{F}^c \cdot \mathbf{F}$ and of a priori unknown but time-independent local material parameters ϑ , i.e.

$$\dot{\vartheta} = 0. \quad (2.18)$$

The function \mathbf{S} will be specified when actual test problems are discussed.

- The fluid component is ideal as the viscosity of the fluid is attributed to the interaction body force $\bar{\pi}^f$, so

$$\sigma^f = -n^f p \mathbf{I}. \quad (2.19)$$

Substitution of (2.16) and (2.19) into (2.12) yields

$$\vec{\nabla} \cdot (\tau^s - p \mathbf{I}) = \vec{0}, \quad (2.20)$$

which is the balance of momentum for the total mixture. From here, τ^s and \vec{q}^s are replaced by τ , respectively \vec{q} .

- The interaction body forces $\bar{\pi}^s$ and $\bar{\pi}^f = -\bar{\pi}^s$ depend linearly on the porosity gradient $\vec{\nabla} n^f$ and on the fluid velocity relative to the solid (Müller [1968], Bowen [1976]), i.e.

$$\bar{\pi}^s = -p \vec{\nabla} n^f + \mathbf{k} \cdot (\vec{v}^f - \vec{v}^s). \quad (2.21)$$

The first term in the right-hand-side of (2.21), the ‘buoyancy force’, originates from the phenomenon that a solid body submerged in a fluid experiences a force proportional to the difference in density between the solid and the fluid. The second term is known as ‘diffusive drag’ and accounts for the viscous effect of the fluid on the solid.

There are several ways to deal with the balance equations (2.15) and (2.20). Here a formulation is used with the solid velocity \vec{v}^s and the fluid pressure p as primary unknown variables. To eliminate the fluid velocity \vec{v}^f , the constitutive models for σ^f and $\bar{\pi}^f$ are substituted in the balance of momentum for the fluid. This results in Darcy’s law

$$n^f (\vec{v}^f - \vec{v}^s) = -\kappa \cdot \vec{\nabla} p, \quad (2.22)$$

where $\kappa = (n^f)^2 \mathbf{k}^{-1}$ is the permeability tensor. The permeability depends on the deformation of the solid. The chosen model, satisfying objectivity, is given by

$$\kappa = \frac{1}{J} \mathbf{F} \cdot \mathbf{K}(J, \underline{\vartheta}) \cdot \mathbf{F}^c, \quad (2.23)$$

where \mathbf{K} is a tensor function of the volume ratio J and the local material parameters $\underline{\vartheta}$. The function \mathbf{K} will be specified when actual test problems are discussed.

- If an initially inhomogeneous mixture is considered, the local material parameters $\underline{\vartheta}$ will vary with the position. It is assumed that the components of $\underline{\vartheta}$ can be written as known functions of the position \vec{x}_0 in the reference configuration and of a set of N_θ unknown constant (i.e. time and position independent) model parameters θ , i.e.

$$\underline{\vartheta} = \psi(\vec{x}_0, \theta). \quad (2.24)$$

When parameter estimation is discussed, it concerns the model parameters θ .

To arrive at unique solutions for the displacements and pressures, specification of boundary conditions at the material surface is required. Boundary conditions may have various forms. In this thesis only straightforward conditions in terms of displacements, pressures, velocities, and stresses will be encountered. Boundary conditions at a surface of discontinuity (Hou *et al.* [1989], Saffman [1971]) or in the case of contact problems (Schreppers [1991], van Lankveld [1994]) will be left out of consideration. If a fluid-solid mixture model is used, boundary conditions can concern either the fluid and solid components separately or both components simultaneously. The current boundary of the solid component of the mixture is denoted by $\mathcal{B}(t)$, the boundary in the reference configuration by $\mathcal{B}_0 = \mathcal{B}(t_0)$.

In solid mechanics a Lagrangian formulation is used and boundary conditions are formulated in terms of quantities that are known in a moving material point. Prescribed solid displacements and velocities are boundary conditions of this type. In fluid mechanics an Eulerian formulation is used and boundary conditions are given in fixed spatial positions. Typical boundary conditions of this type are prescribed pressures and fluid velocities. However, when mixtures are considered, fluid and solid boundary conditions are strongly related, and fluid quantities may be known in material points of the solid.

Let the displacement in the direction of the unit vector \vec{e}_i of a point on the solid boundary be known as a function of time, i.e.

$$\vec{q} \cdot \vec{e}_i = q_i^k(\underline{\psi}), \quad (2.25)$$

where q_i^k is known as a function of the input $\underline{\psi}$. This may happen when the solid is fixed on supports of a given type, or when an indenter is used to deform the solid component. The stress

\vec{t} at the boundary is given by

$$\vec{t} = (\boldsymbol{\tau} - p\mathbf{I}) \cdot \vec{n}, \quad (2.26)$$

where \vec{n} is the unit outward normal on \mathcal{B} . As a rule, the stress \vec{t} is only given on parts of the boundary where \vec{q} is unknown, or perpendicular to the direction in which \vec{q} is prescribed,

$$\vec{t} \cdot \vec{e}_i = t_i^k(\underline{y}), \quad (2.27)$$

where t_i^k is known as a function of \underline{y} in the direction of the unit vector \vec{e}_i . This stress can be carried by both fluid and solid or by the solid component only. The pressure may be given, e.g., at a free surface or at a part of the mixture surface which is in contact with a highly permeable sieve,

$$p = p^k(\underline{y}). \quad (2.28)$$

If $p^k = 0$, the stress is applied to the solid exclusively. Finally, boundary conditions in terms of the fluid velocity relative to the solid are possible. The fluid flow across the boundary per unit of area, s , is equal to

$$s = n^f (\vec{v}^f - \vec{v}^s) \cdot \vec{n}. \quad (2.29)$$

The porosity n^f appears as a result of the averaging procedure. As a rule, s is only given on parts of the boundary where p is unknown,

$$s = s^k(\underline{y}). \quad (2.30)$$

In general, if the fluid flow is prescribed, then it is equal to zero.

Summary:

The relevant equations for a fluid-solid mixture are the total balance of mass

$$\vec{\nabla} \cdot \vec{q} + \vec{\nabla} \cdot (n^f (\vec{v}^f - \vec{v}^s)) = 0, \quad (2.15)$$

and the total balance of momentum

$$\vec{\nabla} \cdot (\boldsymbol{\tau} - p\mathbf{I}) = \vec{0}. \quad (2.20)$$

Since the velocity of the fluid relative to the solid ($\vec{v}^f - \vec{v}^s$) and the pressure p are coupled by Darcy's law

$$n^f (\vec{v}^f - \vec{v}^s) = -\kappa \cdot \vec{\nabla} p, \quad (2.22)$$

the model results in a set of first order partial differential equations in the unknown solid displacement \vec{q} and the unknown fluid pressure p . Precise boundary conditions have not been specified yet as they depend on the actual experiment.

2.3 Solving the model equations

In this section the solution strategy for the model equations will be discussed. Firstly, the equations are spatially discretised by means of the finite element method. This will result in the state-space formulation of the model equations. Secondly, a time discretisation scheme is introduced. Per time point a set of nonlinear algebraic equations results. Finally, these equations are solved using Newton-Raphson iteration.

Although it has been published previously (Oomens *et al.* [1987], Snijders [1994]), a detailed elaboration of the solution strategy is given, because both the finite element method and the Newton-Raphson procedure provide matrices which can be used to study the influence of parameter variations on the displacement and pressure solution analytically. This is especially important for the determination of the sensitivity matrix in the next section. Some matrices will also be used in the optimal estimation algorithm in Chapter 4.

2.3.1 Spatial discretisation

To arrive at a weak formulation of the model equations, (2.15) and (2.20) are premultiplied by weighting functions and integrated over the current mixture volume, according to the weighted residual method. For the actual discretisation, the finite element method is used. The volume is subdivided in a finite number N_e of elements with a relatively simple shape. In each element displacement and pressure nodes are selected. Within each element, the variables \vec{q} and p are approximated by a linear combination of the nodal displacements, respectively nodal pressures. This implies that the original problem of finding $\vec{q}(\vec{x}_0, t)$ and $p(\vec{x}_0, t)$ satisfying the model equations for all $\vec{x}_0 \in \mathcal{C}_0$, is replaced by finding the time-dependent nodal displacements and nodal pressures. According to Galerkin's method, the weighting functions are discretised in the same way as the displacement and pressure field. Then, there are precisely as many nodal weighting variables as unknown nodal displacements and pressures. From the requirement that the weighted residual formulation holds for all possible weighting variables, a set of as many equations as the number of nodal unknowns results. After the boundary conditions are accounted for, a solvable set of equations with a unique solution results (Appendix A)

$$\underline{B} \underline{\dot{q}} + \underline{K} \underline{p} = \underline{s}, \quad (2.31)$$

$$\underline{f} - \underline{B}^T \underline{p} = \underline{t}. \quad (2.32)$$

In this so-called state-space formulation, \underline{q} and \underline{p} are the columns of unknown nodal displacements and nodal pressures. The components of \underline{B} , \underline{K} , \underline{f} , \underline{s} , and \underline{t} are known, smooth, nonlinear

functions of their arguments

$$\underline{B} = \underline{B}(q, u), \quad (2.33)$$

$$\underline{K} = \underline{K}(q, \theta, u), \quad (2.34)$$

$$\underline{s} = \underline{s}(q, \theta, u, \dot{u}), \quad (2.35)$$

$$\underline{f} = \underline{f}(q, \theta, u), \quad (2.36)$$

$$\underline{t} = \underline{t}(q, u). \quad (2.37)$$

The set of model equations (2.31) and (2.32) is completed with the parameter equation (1.2), i.e.

$$\dot{\theta} = 0. \quad (2.38)$$

Initial conditions are required for both q and θ , so

$$\underline{q}(t_0) = \underline{q}_0, \quad \underline{\theta}(t_0) = \hat{\theta}, \quad (2.39)$$

where $\hat{\theta}$ is the a priori estimate of the model parameters. If the parameter equation is satisfied exactly, then it suffices to replace θ in (2.33) to (2.36) by $\hat{\theta}$, and (2.38) can be omitted. However, allowing a residual on the parameter equation induces some freedom in the estimation of the model parameters. Both estimation algorithms presented in this thesis use this possibility.

2.3.2 Determination of the nodal quantities

Equation (2.31) represents a set of nonlinear, ordinary, first order differential equations. It can be solved by standard numerical procedures. Suppose that the solutions q_{j-1} and p_{j-1} of (2.31) and (2.32) at time t_{j-1} are available as a result of previous calculations and that the solutions q_j and p_j at time $t_j = t_{j-1} + \Delta t$ must be determined, for instance because they are used for comparison with measured values at time t_j . If Δt is sufficiently small, then $\dot{q}(t_j)$ can be approximated by means of a simple implicit Euler scheme

$$\dot{q}(t_j) = \frac{1}{\Delta t}(q_j - q_{j-1}). \quad (2.40)$$

Substitution of this approximation in (2.31) and (2.32) results in a set of nonlinear algebraic equations for q_j and p_j , i.e.

$$\frac{1}{\Delta t} \underline{B}_j (q_j - q_{j-1}) + \underline{K}_j p_j = \underline{s}_j, \quad (2.41)$$

$$\underline{f}_j - \underline{B}_j^T p_j = \underline{t}_j, \quad (2.42)$$

where \underline{B}_j , \underline{K}_j , \underline{s}_j , \underline{f}_j , and \underline{t}_j represent (approximated) values at time t_j , so $\underline{B}_j = \underline{B}(q_j, u_j)$, $\underline{K}_j = \underline{K}(q_j, \theta, u_j)$ etc.

For the solution of these equations the Newton-Raphson procedure is used. Let $q_j^{(m)}$ and $p_j^{(m)}$ be available approximations for the solutions q_j and p_j , and let Δq and Δp be the errors in these approximations, so

$$q_j = q_j^{(m)} + \Delta q, \quad p_j = p_j^{(m)} + \Delta p. \quad (2.43)$$

Substitution in (2.41) and (2.42) yields a set of nonlinear algebraic equations in these errors. If Δq and Δp are sufficiently small, then these equations can be linearised, using Taylor's series expansion. Neglecting all terms of second or higher order in Δq and Δp results in a set of linear equations for Δq and Δp , i.e.

$$\left(\frac{1}{\Delta t} \underline{B}_j + \underline{L}_j^{sq} \right) \Delta q + \underline{K}_j \Delta p = r_j^s, \quad (2.44)$$

$$\underline{L}_j^{tq} \Delta q - \underline{B}_j^T \Delta p = r_j^t, \quad (2.45)$$

where the lower index j denotes that the associated quantity must be evaluated with $q = q_j^{(m)}$ and $p = p_j^{(m)}$, for instance $\underline{B}_j = \underline{B}(q_j^{(m)}, u_j)$. The so-called tangential stiffness matrices \underline{L}_j^{sq} and \underline{L}_j^{tq} are discussed in detail in Appendix A. If column k of $\underline{L}^{\alpha\beta}$ is denoted by $(\underline{L}^{\alpha\beta})_k$, then it turns out that

$$(\underline{L}^{sq})_k = \frac{\partial \underline{B}}{\partial q_k} \dot{q} + \frac{\partial \underline{K}}{\partial q_k} p - \frac{\partial \underline{s}}{\partial q_k}, \quad \underline{L}^{sq} = \underline{L}^{sq}(q, \dot{q}, p, \theta, u, \dot{u}), \quad (2.46)$$

$$(\underline{L}^{tq})_k = \frac{\partial f}{\partial q_k} - \frac{\partial t}{\partial q_k}, \quad \underline{L}^{tq} = \underline{L}^{tq}(q, \theta, u), \quad (2.47)$$

so the matrices \underline{L}_j^{sq} and \underline{L}_j^{tq} follow from

$$\underline{L}_j^{sq} = \underline{L}^{sq} \left(q_j^{(m)}, \frac{1}{\Delta t} (q_j^{(m)} - q_{j-1}), p_j^{(m)}, \theta, u_j, \dot{u}_j \right), \quad (2.48)$$

$$\underline{L}_j^{tq} = \underline{L}^{tq} \left(q_j^{(m)}, \theta, u_j \right). \quad (2.49)$$

Finally, the residuals r_j^s and r_j^t in (2.44) and (2.45) are defined by

$$r_j^s = \underline{s}_j - \frac{1}{\Delta t} \underline{B}_j (q_j^{(m)} - q_{j-1}) - \underline{K}_j p_j^{(m)}, \quad (2.50)$$

$$r_j^t = t_j - f_j + \underline{B}_j^T p_j^{(m)}. \quad (2.51)$$

Solving (2.44) and (2.45) for Δq and Δp results in approximations for these errors. Substitution of the obtained values in $q_j^{(m+1)} = q_j^{(m)} + \Delta q$ and in $p_j^{(m+1)} = p_j^{(m)} + \Delta p$ yields new approximations for the solutions q_j and p_j of (2.41) and (2.42). The iteration process is repeated until a predefined number of iterations has been executed or until some measure of the errors or of the residuals has become smaller than a predefined value $\varepsilon > 0$. Possible criteria are given by Bathe [1982].

To start the iteration process, initial approximations $q_j^{(1)}$ and $p_j^{(1)}$ must be specified. Here, the solutions q_{j-1} and p_{j-1} for the previous time point $t_{j-1} = t_j - \Delta t$ are used, so

$$q_j^{(1)} = q_{j-1}, \quad p_j^{(1)} = p_{j-1}. \quad (2.52)$$

2.3.3 Parameter variations

The numerical procedure of the previous section can be used only if a set $\underline{\theta}$ of parameters is given. However, the parameters are unknown a priori. For future investigations it is important to analyse the influence of parameter variations on the nodal displacements and the nodal pressures.

As before, let $\underline{q}(t)$ and $\underline{p}(t)$ be the nodal quantities at time $t > t_i$ corresponding to an initial condition $\underline{q}(t_i) = \underline{q}_i$, an input $\underline{u}(\tau) \mid \tau \in [t_i, t]$ and a chosen set of parameters $\underline{\theta}$. Furthermore, let $\underline{q}(t) + \delta\underline{q}(t)$ and $\underline{p}(t) + \delta\underline{p}(t)$ be the nodal quantities at time t for the situation with the same initial condition and the same input but with parameters $\underline{\theta} + \delta\underline{\theta}$ instead of $\underline{\theta}$. Only infinitesimal small variations $\delta\underline{\theta}$ are considered. It can be shown that the variations $\delta\underline{q}$ and $\delta\underline{p}$ of the nodal quantities are proportional to $\delta\underline{\theta}$, i.e.

$$\delta\underline{q}(t) = \underline{Q}(t)\delta\underline{\theta}, \quad \delta\underline{p}(t) = \underline{P}(t)\delta\underline{\theta}. \quad (2.53)$$

From (2.31) to (2.37) it is readily seen that the matrices \underline{Q} and \underline{P} can be determined from

$$\underline{B} \underline{\dot{Q}} + \underline{L}^{sq} \underline{Q} + \underline{K} \underline{P} = -\underline{L}^{s\theta}, \quad (2.54)$$

$$\underline{L}^{tq} \underline{Q} - \underline{B}^T \underline{P} = -\underline{L}^{t\theta}, \quad (2.55)$$

with the initial condition $\underline{Q}(t_i) = \underline{Q}$. The matrices \underline{L}^{sq} and \underline{L}^{tq} are defined earlier in (2.46) and (2.47). The components of the matrices $\underline{L}^{s\theta}$ and $\underline{L}^{t\theta}$ represent derivatives with respect to the parameters. If column k of $\underline{L}^{\alpha\theta}$ is denoted by $(\underline{L}^{\alpha\theta})_k$, then

$$(\underline{L}^{s\theta})_k = \frac{\partial \underline{K}}{\partial \theta_k} \underline{p} - \frac{\partial \underline{S}}{\partial \theta_k}, \quad \underline{L}^{s\theta} = \underline{L}^{s\theta}(\underline{q}, \underline{p}, \underline{\theta}, \underline{u}, \dot{\underline{u}}), \quad (2.56)$$

$$(\underline{L}^{t\theta})_k = \frac{\partial \underline{f}}{\partial \theta_k}, \quad \underline{L}^{t\theta} = \underline{L}^{t\theta}(\underline{q}, \underline{\theta}, \underline{u}). \quad (2.57)$$

For the actual calculation of $\underline{Q}_j = \underline{Q}(t_j)$ and $\underline{P}_j = \underline{P}(t_j)$ at time $t_j = t_{j-1} + \Delta t$ again the simple implicit Euler scheme is used. This immediately results in

$$\left(\frac{1}{\Delta t} \underline{B}_j + \underline{L}_j^{sq} \right) \underline{Q}_j + \underline{K}_j \underline{P}_j = -\underline{L}_j^{s\theta} + \frac{1}{\Delta t} \underline{B}_j \underline{Q}_{j-1}, \quad (2.58)$$

$$\underline{L}_j^{tq} \underline{Q}_j - \underline{B}_j^T \underline{P}_j = -\underline{L}_j^{t\theta}. \quad (2.59)$$

2.3.4 Concluding remarks

There is great similarity between the equations (2.44) and (2.45) for the columns $\Delta\underline{q}$ and $\Delta\underline{p}$ and the equations (2.58) and (2.59) for the matrices \underline{Q}_j and \underline{P}_j . As a consequence, the matrices used in Section 2.3.2 to determine \underline{q}_j and \underline{p}_j can also be used for the calculation of \underline{Q}_j and \underline{P}_j . Hence,

as soon as \underline{q}_j and \underline{p}_j are known, both \underline{Q}_j and \underline{P}_j can be determined with very little effort.

Until now, hardly any attention is given to the matrices $\underline{L}^{s\theta}$ and $\underline{L}^{t\theta}$ in the right hand side of equation (2.58) and equation (2.59). A more detailed discussion on these matrices can be found in Appendix A.

In Section 2.3.2 and Section 2.3.3 it is assumed that the length Δt of the time interval $[t_{j-1}, t_j]$ is small enough, so that an implicit Euler scheme of the type of (2.40) can be applied. If Δt is too large, then this scheme will yield unacceptable results for \underline{q}_j , \underline{p}_j , \underline{Q}_j and \underline{P}_j . In that case the considered interval is divided in $k > 1$ subintervals and the procedures of Section 2.3.2 and Section 2.3.3 are applied per subinterval.

2.4 The output equation and the sensitivity matrix

2.4.1 The output equation

For the estimation of the a priori unknown model parameters, measured values of system quantities are confronted with the calculated values of these quantities. The calculated quantities are seen as the components of the output \underline{y} . Since only displacements and pressures are measured, the model output at time t is a function of the nodal displacements $\underline{q}(t)$, the nodal pressures $\underline{p}(t)$ and the input $\underline{u}(t)$, i.e.

$$\underline{y} = \underline{g}(\underline{q}, \underline{p}, \underline{u}). \quad (2.60)$$

Measurements are only performed at a finite number of discrete points of time t_1, t_2, \dots . The measured value of the output at time t_{i+1} is denoted by \underline{m}_{i+1} whereas the value of the output as calculated with the model is denoted by \underline{y}_{i+1} , so

$$\underline{y}_{i+1} = \underline{g}(\underline{q}_{i+1}, \underline{p}_{i+1}, \underline{u}_{i+1}). \quad (2.61)$$

As shown in the previous section, it is possible to calculate \underline{q}_{i+1} and \underline{p}_{i+1} for $t_{i+1} > t_i$ as soon as the initial condition $\underline{q}_i = \underline{q}(t_i)$, the input $\underline{u}(\tau) \mid \tau \in [t_i, t_{i+1}]$ and a value for the parameters $\underline{\theta}$ are given.

2.4.2 The sensitivity matrix

A variation $\delta\theta$ of the parameters will result in a variation $\delta\underline{y}_{i+1}$ of the model output \underline{y}_{i+1} at time t_{i+1} . From equation (2.61) it is seen that

$$\delta\underline{y}_{i+1} = \underline{G}_{i+1}^q \delta\underline{q}_{i+1} + \underline{G}_{i+1}^p \delta\underline{p}_{i+1}, \quad (2.62)$$

where the matrices \underline{G}^q and \underline{G}^p represent the derivatives of the output with respect to the nodal displacements, respectively the nodal pressures. Using equation (2.53) it is readily seen that

$$\delta \underline{y}_{i+1} = \underline{H}_{i+1} \delta \underline{\theta}, \quad \underline{H}_{i+1} = \underline{G}_{i+1}^q \underline{Q}_{i+1} + \underline{G}_{i+1}^p \underline{P}_{i+1}. \quad (2.63)$$

The sensitivity matrix \underline{H} plays an important role in the procedures to determine the model parameters.

The actual determination of the components of the sensitivity matrix \underline{H}_{i+1} at time t_{i+1} can be done by numerical differentiation. Then, first the output \underline{y}_{i+1} is calculated by solving the model equations (2.31) and (2.32) over the time interval $[t_i, t_{i+1}]$, using the given initial condition $\underline{q}(t_i) = \underline{q}_i$, the given input $\underline{u}(\tau) \mid \tau \in [t_i, t_{i+1}]$ and a given set $\underline{\theta}$ of parameters. Next, the parameters are varied one by one and for each varied parameter the model equations are solved over $[t_i, t_{i+1}]$, using the given initial condition and the given input but with the varied parameters. If parameter θ_k is varied, then the difference between varied output and the original output, divided by the value of the variation $\delta \theta_k$, is equal to column k of the sensitivity matrix \underline{H}_{i+1} . This approach to determine \underline{H}_{i+1} is straightforward but very time-consuming.

A much more efficient approach is to use (2.63) for \underline{H}_{i+1} where \underline{Q}_{i+1} and \underline{P}_{i+1} are calculated with the algorithm from Section 2.3.3. This so-called pseudo-analytical approach (Hsieh and Arora [1985], Haug *et al.* [1986], Kulkarni and Noor [1995]) will be used here. It is implemented in the commercial finite element code DIANA (de Borst *et al.* [1985]).

A fast technique to determine the sensitivity is not only valuable during estimation. It is also important to study the sensitivity in the numerical model of the experiment before starting the estimation procedure, as sensitivity is strongly related to identifiability of parameters. If the sensitivity for a specific parameter in an experiment is very low, then the measurements contain little information with respect to that parameter. Therefore, sensitivities are also valuable in designing test procedures (Laible *et al.* [1994]). Sensitivity analyses can also be used to reveal interdependencies between parameters: if two or more columns of the sensitivity matrix are approximately dependent, then the corresponding parameters are highly correlated and the material model may be over-parameterised (Yin *et al.* [1986]).

Chapter 3

A recursive estimation algorithm

3.1 Introduction

The parameters have to be determined such that the model output corresponds to the measurements as good as possible. For this purpose a scalar measure of the residuals between model output and measurements is minimised, while the model equations are satisfied exactly. The estimation algorithm primarily depends on the choice for the scalar measure. This chapter deals with a *recursive estimation algorithm*, which is very efficient.

A modified weighted squares measure of the residuals is introduced in Section 3.2. At each time point where measurements become available, the difference between the model output and the current measurements is weighted and squared, and the weighted square of the difference between the current and the previous parameter estimates is added to account for information in the parameters as a result of previous measurements.

Minimisation of this measure with respect to the parameters leads to a set of nonlinear algebraic equations in the current estimate. The solution to this problem and the choice of the weighting matrices are discussed in Section 3.3.

The efficiency of the estimation algorithm results from the fact that, to determine the output at the current time point, the model equations do not have to be solved over the total time interval up to the current time point, but only over the last time step. Also contributing to efficiency is the use of the pseudo-analytical technique to determine the sensitivity matrix.

The proposed recursive algorithm is applied in Section 3.4 to simulations of an 'experiment' with a two-component fluid-solid mixture. The influence of 'measurement' and model errors on estimation is studied.

3.2 The determination of parameters

It is assumed that displacement and pressure measurements at a number of points on the boundary and inside the material are available at N subsequent points of time t_1, t_2, \dots, t_N . At each point of time the same quantities are measured. All measurements at time t_i are stored in a column \underline{m}_i . The objective is to find estimates of \underline{q} , \underline{p} , and $\underline{\theta}$ that satisfy the model equations (2.31) and (2.32) and that minimise the difference between the model output \underline{y}_i and the measured output \underline{m}_i for $i \in \{1, \dots, N\}$.

3.2.1 The method of least squares

The weighted squares measure J_N for the residuals $\zeta_i = \underline{m}_i - \underline{y}_i$, $i \in \{1, \dots, N\}$ is given by

$$J_N = \sum_{i=1}^N (\underline{m}_i - \underline{y}_i)^T \underline{V}_i (\underline{m}_i - \underline{y}_i), \quad (3.1)$$

where \underline{V}_i is a symmetric, (semi-) positive definite weighting matrix. By incorporating a weighting matrix in this measure, it is possible to account for differences in confidence between measurements at distinct time points or between distinct measurement components. The measure satisfies the requirement that if $J_N = 0$ then $\underline{y}_i = \underline{m}_i$ for all $i \in \{1, \dots, N\}$. The estimate $\hat{\underline{\theta}}$ of $\underline{\theta}$ has to minimise J_N under the constraint that the model equations are satisfied for all $t \in [t_0, t_N]$. Minimisation of J_N requires the variation δJ of J_N to be equal to 0 for all variations $\delta \underline{\theta}$ of $\underline{\theta}$. This necessary but not sufficient requirement leads to a nonlinear set of algebraic equations in $\underline{\theta}$, which is solved by an iterative procedure. For every iteration step the model equations have to be solved over the interval $[t_0, t_N]$. Therefore, estimation will require much computational effort. Moreover, all measurements have to be available during the total procedure, and this requires a large amount of computer memory.

The method has another disadvantage. It assumes that only measurement errors occur and that the model equations are satisfied exactly. It would be more realistic to take model errors into account by allowing residuals on the model equations also. These residuals can be included into J_N (van de Molengraft [1990]). In Chapter 4 an estimation algorithm of this type will be described.

3.2.2 The recursive approach

Suppose that, in one way or another, at time point t_r ($r < N$) an estimate $\hat{\underline{\theta}}_r$ has been determined from the measurements $\underline{m}_1, \dots, \underline{m}_r$. A new measurement \underline{m}_{r+1} of the output becomes available at time t_{r+1} and a new estimate $\hat{\underline{\theta}}_{r+1}$ can be determined by minimising the scalar measure

$$J_{r+1} = \sum_{i=1}^{r+1} (\underline{m}_i - \underline{y}_i)^T \underline{V}_i (\underline{m}_i - \underline{y}_i), \quad (3.2)$$

where \underline{V}_i is a symmetric, (semi-) positive definite weighting matrix. An estimation procedure, based on minimisation of this measure, requires that the model equations are solved over the total interval $[t_0, t_{r+1}]$, possibly many times if an iterative procedure has to be used to solve this nonlinear minimisation problem.

A more efficient procedure will result if it is possible to determine a new estimate $\hat{\underline{\theta}}_{r+1}$ at time point t_{r+1} , starting from the previous estimate $\hat{\underline{\theta}}_r$ and the earlier calculated nodal displacements \underline{q}_r and pressures \underline{p}_r at time t_r . Then, the model equations only have to be solved over the last time step $[t_r, t_{r+1}]$ instead of over the total interval $[t_0, t_{r+1}]$ for each iteration.

Starting point for such a recursive approach is the assumption that the estimate $\hat{\underline{\theta}}_r$ is fairly reliable and that the reliability of $\hat{\underline{\theta}}_r$ increases with the number r of measurements that have been used for estimation. Then, the estimate $\hat{\underline{\theta}}_{r+1}$ on the basis of one more measurement will not deviate much from $\hat{\underline{\theta}}_r$. This is in agreement with the requirement that the parameter equation $\hat{\underline{\theta}} = \underline{\theta}$ has to be satisfied as good as possible. Based on these considerations, a modified weighted squares measure J_{r+1}^* is introduced instead of J_{r+1}

$$J_{r+1}^* = (\underline{\theta} - \hat{\underline{\theta}}_r)^T \underline{W}_{r+1} (\underline{\theta} - \hat{\underline{\theta}}_r) + (\underline{m}_{r+1} - \underline{y}_{r+1})^T \underline{V}_{r+1} (\underline{m}_{r+1} - \underline{y}_{r+1}). \quad (3.3)$$

With the weighting matrices \underline{V}_{r+1} and \underline{W}_{r+1} it is possible to balance between the confidence in the previous parameter estimate $\hat{\underline{\theta}}_r$ and in the new information in the measurements \underline{m}_{r+1} . \underline{V}_{r+1} is symmetric, (semi-) positive definite and \underline{W}_{r+1} is symmetric, positive definite. The modified measure J_{r+1}^* expresses the objective of finding $\hat{\underline{\theta}}_{r+1}$ such that the difference with the previous estimate is as small as possible, while the model output \underline{y}_{r+1} matches the measurements \underline{m}_{r+1} at t_{r+1} as good as possible. In general, minimisation of J_{r+1}^* results in another value of the parameters than minimisation of J_{r+1} .

Minimisation of J_{r+1}^* requires the calculation of the model output \underline{y}_{r+1} and the sensitivity \underline{H}_{r+1} of the model output with respect to the model parameters. The output \underline{y}_{r+1} is a function of the nodal displacements \underline{q}_{r+1} , the nodal pressures \underline{p}_{r+1} and the input \underline{u}_{r+1} according to (2.61)

$$\underline{y}_{r+1} = \underline{g}(\underline{q}_{r+1}, \underline{p}_{r+1}, \underline{u}_{r+1}). \quad (3.4)$$

At t_r , a solution for the nodal displacements \underline{q}_r is available on the basis of the previous estimate $\hat{\underline{\theta}}_r$. As shown in Section 2.3.2, \underline{q}_{r+1} and \underline{p}_{r+1} can be determined by solving the model equations (2.31) and (2.32) with initial condition $\underline{q}(t_r) = \underline{q}_r$, the input $\underline{u}(\tau) \mid \tau \in [t_r, t_{r+1}]$ and a value for the parameters $\underline{\theta}$. Since the input is known and variations of \underline{q}_r do not occur, this is denoted by

$$\underline{y}_{r+1} = \underline{\gamma}_{r+1}(\underline{\theta}). \quad (3.5)$$

This equation expresses the fact that it is possible to compute \underline{y}_{r+1} given a set of parameters $\underline{\theta}$. The sensitivity matrix \underline{H}_{r+1} is computed by means of (2.62)

$$\underline{H}_{r+1} = \underline{G}_{r+1}^q \underline{Q}_{r+1} + \underline{G}_{r+1}^p \underline{P}_{r+1}, \quad (3.6)$$

where \underline{Q}_{r+1} and \underline{P}_{r+1} are determined by solving (2.54) and (2.55) with initial condition $\underline{Q}_r = \underline{Q}$. Main advantage of the recursive approach is that the model equations only have to be solved over the interval $[t_r, t_{r+1}]$ instead of over the total interval $[t_0, t_{r+1}]$ to obtain \underline{y}_{r+1} and \underline{H}_{r+1} .

3.3 The recursive estimation algorithm

3.3.1 Solving the minimisation problem

The requirement that $\hat{\underline{\theta}}_{r+1}$ minimises J_{r+1}^* leads to a set of nonlinear algebraic equations

$$\underline{W}_{r+1} (\underline{\theta} - \hat{\underline{\theta}}_r) - \underline{H}_{r+1}^T \underline{V}_{r+1} (\underline{m}_{r+1} - \underline{y}_{r+1}) = \underline{0}, \quad (3.7)$$

which resembles a Luenberger observer (Luenberger [1966]). To determine $\hat{\underline{\theta}}_{r+1}$, an iterative procedure is required. The new approximation $\hat{\underline{\theta}}_{r+1}^{(l+1)}$ in iteration step l is written as the sum of the approximation in iteration step l plus a correction term, i.e.

$$\hat{\underline{\theta}}_{r+1}^{(l+1)} = \hat{\underline{\theta}}_{r+1}^{(l)} + \Delta \underline{\theta}, \quad (3.8)$$

where $\hat{\underline{\theta}}_r$ is used as the initial approximation $\hat{\underline{\theta}}_{r+1}^{(1)}$ of $\hat{\underline{\theta}}_{r+1}$, so

$$\hat{\underline{\theta}}_{r+1}^{(1)} = \hat{\underline{\theta}}_r. \quad (3.9)$$

Substitution of (3.8) in (3.7) results in a set of nonlinear equations in the unknown $\Delta \underline{\theta}$. These equations are linearised, using Taylor's series expansion of $\underline{y}_{r+1} = \underline{\gamma}_{r+1}(\underline{\theta})$ around $\hat{\underline{\theta}}_{r+1}^{(l)}$ and neglecting all terms of second or higher order in $\Delta \underline{\theta}$. Also the sensitivity matrix \underline{H}_{r+1} should be linearised. As this would lead to the use of three-dimensional matrices, while no significant contribution to the speed of convergence of the iterative procedure is expected, a zero order approximation is applied for this matrix. Finally, a set of linear algebraic equations results

$$\underline{A}_{r+1} \Delta \underline{\theta} = \underline{\rho}_{r+1}, \quad (3.10)$$

where \underline{A}_{r+1} and $\underline{\rho}_{r+1}$ are given by

$$\underline{A}_{r+1} = \underline{W}_{r+1} + \underline{H}_{r+1}^T \underline{V}_{r+1} \underline{H}_{r+1}, \quad (3.11)$$

$$\rho_{r+1} = \underline{H}_{r+1}^T \underline{V}_{r+1} \left(\underline{m}_{r+1} - \gamma_{r+1} (\hat{\theta}_{r+1}^{(l)}) \right) - \underline{W}_{r+1} \left(\hat{\theta}_{r+1}^{(l)} - \hat{\theta}_r \right). \quad (3.12)$$

As \underline{W}_{r+1} is positive definite and \underline{V}_{r+1} is at least semi-positive definite, \underline{A}_{r+1} will be positive definite. Therefore, $\Delta \hat{\theta}$ can be solved from equation (3.10) and $\hat{\theta}_{r+1}^{(l+1)}$ can be determined. The iteration process is repeated until a predefined number of iterations has been executed or until a suitable measure of the correction term or of the right-hand side of (3.10) has become smaller than a predefined value $\varepsilon_\theta > 0$.

The estimation scheme used by Hendriks [1991] resembles equation (3.10). However, Hendriks did not distinguish between $\hat{\theta}_{r+1}^{(l)}$ and $\hat{\theta}_r$ and it was therefore not possible to perform iterations within one time step.

3.3.2 Specification of the weighting matrices

A possible choice for the weighting matrices is based on the assumption that the reliability of the current estimate $\hat{\theta}_{r+1}$ depends on the reliability of the measurement \underline{m}_{r+1} and the reliability of the previous estimate $\hat{\theta}_r$.

Let $\delta \hat{\theta}_{r+1}$ be the variation of $\hat{\theta}_{r+1}$ as a result of a small perturbation \underline{v}_{r+1} on \underline{m}_{r+1} and a small perturbation $\delta \hat{\theta}_r$ on $\hat{\theta}_r$. The varied solution $\hat{\theta}_{r+1} + \delta \hat{\theta}_{r+1}$ has to satisfy equation (3.7). Elaboration of this equation, neglecting terms of second or higher order in $\delta \hat{\theta}_{r+1}$, yields

$$\underline{A}_{r+1} \delta \hat{\theta}_{r+1} = \underline{H}_{r+1}^T \underline{V}_{r+1} \underline{v}_{r+1} + \underline{W}_{r+1} \delta \hat{\theta}_r. \quad (3.13)$$

Let \underline{S}_{r+1}^m be a quadratic measure of \underline{v}_{r+1} and let \underline{S}_r^θ be a corresponding quadratic measure of $\delta \hat{\theta}_r$. If the cross-products $\underline{v}_{r+1} \delta \hat{\theta}_r^T$ and $\delta \hat{\theta}_r \underline{v}_{r+1}^T$ are neglected, $\underline{S}_{r+1}^\theta$ will satisfy

$$(\underline{A}_{r+1} \underline{S}_{r+1}^\theta \underline{A}_{r+1}^T) = (\underline{H}_{r+1}^T \underline{V}_{r+1} \underline{S}_{r+1}^m \underline{V}_{r+1}^T \underline{H}_{r+1}) + (\underline{W}_{r+1} \underline{S}_r^\theta \underline{W}_{r+1}^T). \quad (3.14)$$

If the reliability of \underline{m}_{r+1} is high, then only small perturbations \underline{v}_{r+1} will occur. In that case, the norm of \underline{S}_{r+1}^m is small. Likewise, the norm of \underline{S}_r^θ is small if the previous estimate is reliable. Moreover, \underline{S}^m is constant if subsequent measurements are equally reliable, $\underline{S}_{r+1}^m = \underline{S}^m$.

As mentioned earlier, the weighting matrices \underline{V}_{r+1} and \underline{W}_{r+1} have to express the confidence in the quality of the measurements, respectively of the prior estimate $\hat{\theta}_r$. The norm of \underline{V}_{r+1} and \underline{W}_{r+1} has to be large if confidence is high. Therefore, it is likely to choose

$$\underline{V}_{r+1} = (\underline{S}^m)^{-1}, \quad \underline{W}_{r+1} = (\underline{S}_r^\theta)^{-1}. \quad (3.15)$$

With these choices for \underline{V}_{r+1} and \underline{W}_{r+1} , $\underline{S}_{r+1}^\theta$ can be determined from

$$\underline{S}_{r+1}^\theta = \underline{A}_{r+1}^{-1} = \left(\underline{H}_{r+1}^T (\underline{S}^m)^{-1} \underline{H}_{r+1} + (\underline{S}_r^\theta)^{-1} \right)^{-1}, \quad (3.16)$$

where (3.15), (3.14) and (3.11) are used. It is noted that \underline{V}_{r+1} is constant while \underline{W}_{r+1} has to be updated after each measurement.

Let \underline{m}_{r+1} and $\hat{\underline{\theta}}_r$ be realisations of random variables and let \underline{v}_{r+1} and $\delta\hat{\underline{\theta}}_r$ be realisations of a zero mean normal distribution. As a quadratic measure of \underline{v}_{r+1} and $\delta\hat{\underline{\theta}}_r$, the variance \underline{S}^m of the measurements \underline{m}_{r+1} , respectively the variance \underline{S}_r^θ of the parameters $\hat{\underline{\theta}}_r$ can be used. Then, $\underline{S}_{r+1}^\theta$ according to (3.16) is the variance of $\hat{\underline{\theta}}_{r+1}$, and a Kalman-like estimator results.

Hendriks [1991] and van Ratingen [1994] already pointed out that in some applications the actual error on the parameter estimates exceeds the value that is predicted by the updated variance $\underline{S}_{r+1}^\theta$. If $\underline{S}_{r+1}^\theta$ is too small, parameters will converge slowly. In that case, Hendriks proposes to replace $\underline{S}_{r+1}^\theta$ by the sum of $\underline{S}_{r+1}^\theta$ and a small, constant, symmetric positive definite matrix (Anderson and Moore [1973]).

In Appendix B the recursive estimation procedure, including the pseudo-analytical determination of the sensitivity matrix, is summarised. Implementation of the recursive estimation algorithm in DIANA required some adaptations to the module PAREST, the parameter estimation facility of DIANA (TNO Building and Construction Research [1993], Hendriks [1991]).

3.4 Testing of the recursive algorithm

To test the recursive algorithm, laboratory experiments and numerical experiments with fluid-solid mixtures are required. Performing laboratory experiments is an essential step in the evaluation of an identification technique, as both unknown model errors and measurement errors occur. Simulations give the opportunity to separately study the effect of model and measurement errors on the identification of the parameters. In the present research, only simulations are performed to test the proposed algorithm.

After the constitutive behaviour is discussed, the set-up of the ‘experiment’ is described and a finite element model is introduced. For the generation of the ‘experimental’ data and for the numerical analyses during identification, the same finite element model is used to avoid model errors due to the mesh. Two tests will be performed. In the first test, the influence of measurement errors is studied by adding noise to the generated data. During this test, no model errors are present. In the second test, a model error is introduced.

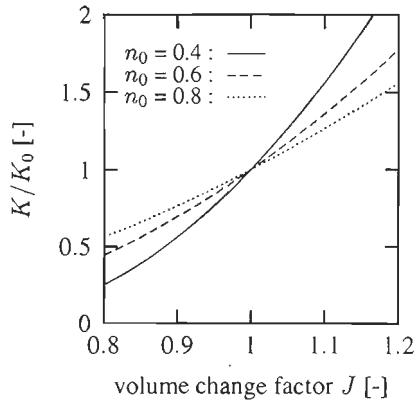


Figure 3.1: Dependency of the permeability K on deformation according to Huyghe [1986].

3.4.1 Constitutive behaviour

The numerical-experimental technique allows the use of inhomogeneous and anisotropic materials. Nevertheless, an initially homogeneous, isotropic fluid-solid mixture is considered here. Therefore, the local material parameters ϑ are independent of the position in the material and equation (2.24) reduces to

$$\vartheta = \theta. \tag{3.17}$$

For the elastic solid (2.17), a linear relation between the second Piola-Kirchhoff stress tensor \mathbf{S} and the Green-Lagrange strain tensor \mathbf{E} is assumed (Fung [1965], Hunter [1983])

$$\mathbf{S} = 2\mu \mathbf{E} + \lambda \operatorname{tr}(\mathbf{E}) \mathbf{I}, \quad \mathbf{E} = \frac{1}{2}(\mathbf{C} - \mathbf{I}), \tag{3.18}$$

where \mathbf{I} is the second order unit tensor and the Lamé constants λ and μ are related to Young’s modulus E and Poisson’s ratio ν by

$$\lambda = \frac{E\nu}{(1 + \nu)(1 - 2\nu)}, \quad \mu = \frac{E}{2(1 + \nu)}. \tag{3.19}$$

As the mixture is isotropic, the permeability is independent of the material direction, so

$$\mathbf{K} = K \mathbf{I}. \tag{3.20}$$

The permeability scalar K is assumed to depend on the volume ratio J of current state and reference state according to

$$K = K_0 \left(\frac{J - 1}{n_0} + 1 \right)^2, \tag{3.21}$$

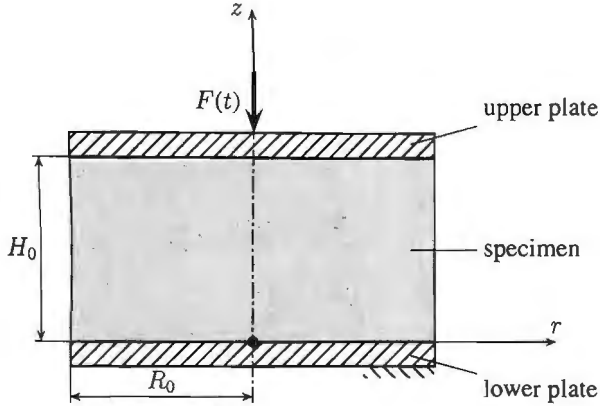


Figure 3.2: 'Experimental' set-up.

where K_0 is the initial permeability and n_0 is the initial porosity of the mixture (Huyghe [1986]). In Figure 3.1, the influence of n_0 and J on the permeability according to (3.21) is given. With (3.19) and (3.21), the column of a priori unknown model parameters becomes

$$\theta = [E, \nu, K_0, n_0]^T. \quad (3.22)$$

3.4.2 'Experimental' set-up

Both ends of a cylindrical specimen, with initial height $H_0 = 1$ and radius $R_0 = 1$, are attached to rigid impermeable solid plates (Figure 3.2). A time-dependent load $F(t)$ is applied to the upper plate along the symmetry-axis of the mixture. The lower plate is fixed on a rigid foundation. Fluid flow across the free boundary surface is allowed.

As the material is assumed to be homogeneous, an axi-symmetric problem results. A vector base $\langle \vec{e}_r, \vec{e}_\phi, \vec{e}_z \rangle$ with origin \mathcal{O} and unit vector \vec{e}_z along the symmetry-axis of the specimen is introduced. In the figure, the origin \mathcal{O} is marked with a dot. With this base, the displacement vector \vec{q} can be written as

$$\vec{q} = q_r \vec{e}_r + q_z \vec{e}_z, \quad (3.23)$$

where q_r is the radial displacement and q_z is the axial displacement. The tangential displacement q_ϕ is equal to zero and q_r, q_z and the pressure p do not depend on the circumferential coordinate ϕ . At the lower plate, the displacements in r and z -direction are suppressed, i.e.

$$q_r(r_0, z_0 = 0, t) = 0, \quad q_z(r_0, z_0 = 0, t) = 0. \quad (3.24)$$

nr.	r_0	z_0	position
1	0.0	0.0	at lower plate
2	0.36	0.0	
3	0.64	0.0	
4	1.0	0.25	at free surface
5	1.0	0.5	
6	1.0	0.75	
7	0.0	1.0	at upper plate

Table 3.1: The positions of the measurement points

The displacements at the upper plate are suppressed in r -direction, so

$$q_r(r_0, z_0 = H_0, t) = 0. \quad (3.25)$$

At the free boundary surface the pressure is assumed to be equal to zero, i.e.

$$p(r_0 = R_0, z_0, t) = 0. \quad (3.26)$$

The measurements have to offer sufficient information to allow a unique identification of the model parameters. For this reason, both displacement and pressure measurements are used (Op den Camp *et al.* [1994]). The measured quantities are the axial displacement of the upper plate (point 7 in Table 3.1), the radial and axial displacements of three points at the outer surface of the specimen (points 4, 5 and 6 in Table 3.1), and the pressure in three points at the interface with the lower plate (points 1, 2, and 3 in Table 3.1). The ‘measurements’ are performed at 100 equally distributed points in the time interval $[0, 1]$.

3.4.3 Finite element analysis

For the generation of measurement data, a finite element analysis is performed with an arbitrarily chosen set $\bar{\theta}$ of parameters,

$$\bar{\theta} = [1.0, 0.4, 1.0, 0.8]^T. \quad (3.27)$$

This set will be called the true parameter set. The specimen is modelled in DIANA (de Borst *et al.* [1985]) by means of 144, isoparametric, 4-noded, axi-symmetric, mixture elements. The nodal displacements at the lower plate are suppressed in radial and axial direction. The nodal displacements at the upper plate are suppressed in radial direction and tied in axial direction to take into account that the upper plate is rigid. The nodal displacements at the symmetry-axis are

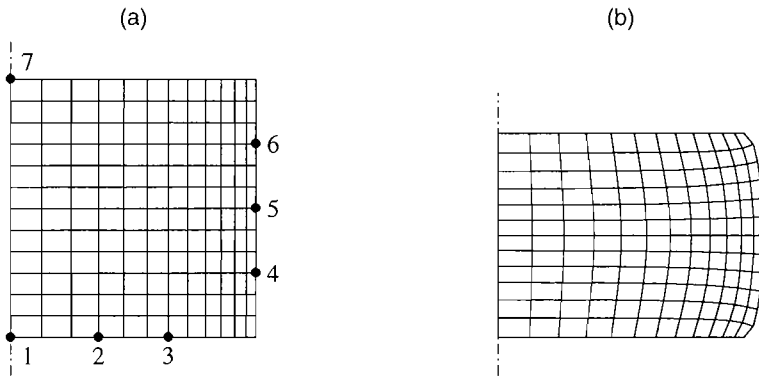


Figure 3.3: The finite element mesh in the undeformed state (a) and in the deformed state (b).

suppressed in radial direction. At the free boundary surface, the pressure is equal to zero. The compressive load F on the mixture is a function of time with $F(t) = 0$ for $t < 0$. From $t = 0$ to $t = 1$ the load is applied according to Figure 3.4(a). Finally, $F(t) = 0$ for $t > 1$. With a maximum load $F = 0.5$, a maximum Green-Lagrange strain of about 0.2 is achieved. For the time-discretisation, 100 equal time steps are used over the interval $[0, 1]$.

Figure 3.3 depicts the finite element model before loading –the undeformed state– and after consolidation when the pressure is equal to zero and the total external load is carried by the solid. The measurement points are marked with a dot. The resulting displacements and pressures in the measurement points are shown in Figure 3.4 (b–d). During loading, the pressure increases and a negative pressure gradient occurs in the radial direction. According to Darcy’s law (2.22), fluid flows in positive radial direction and is squeezed out of the mixture. Due to deformation, elastic energy is stored into the solid. When the specimen is gradually unloaded ($0.25 < t \leq 0.5$), the pressure decreases fast to negative values as the solid starts to regain its original shape and the elastic energy is released. A positive pressure gradient occurs and the fluid is sucked back into the mixture. At $t = 0.5$, when the load is equal to zero, the pressure gradient even causes the radial displacement to be slightly negative. For $0.5 < t < 1$, the same phenomena as described above occur.

The results in the measurement points 1 – 7 will be used as observations for the estimation process. The components of the column of measurements m_i at time t_i ($i \in \{1, \dots, 100\}$) are 3 pressures, 3 radial displacements and 4 axial displacements. In addition to the case of perfect observations, estimations are performed with artificially disturbed data. To each element of the computed data, a realisation of a zero mean normal distribution is added. The standard deviation

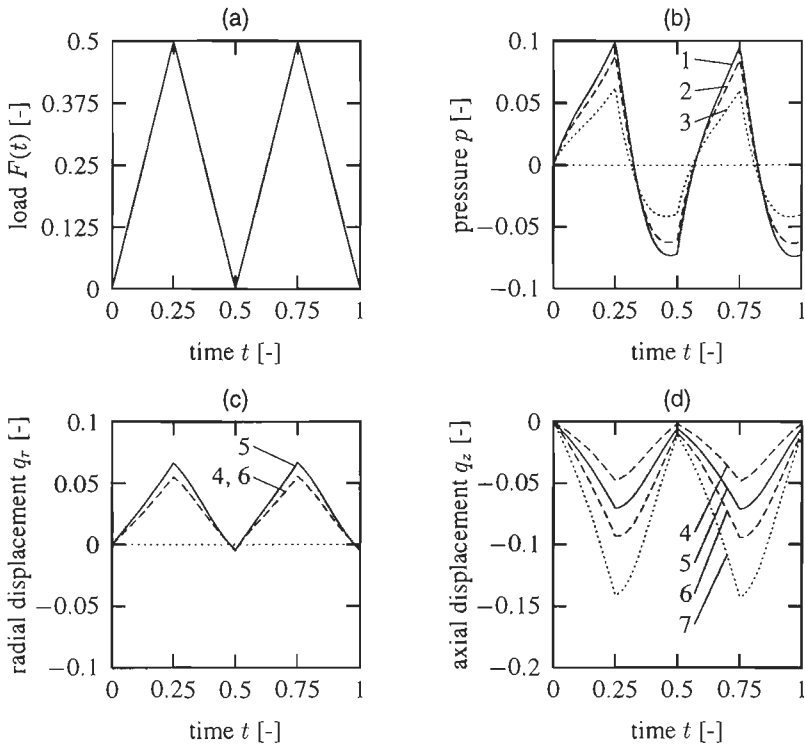


Figure 3.4: Analysis of the 'experiment': (a) the applied compressive load on the specimen versus time; (b) the pressure $p(t)$ in 1, 2 and 3; (c) the radial displacement $q_r(t)$ of 4, 5 and 6; (d) the axial displacement $q_z(t)$ of 4, 5, 6 and 7.

Parameters		Initial guess		Estimation results			True value
$(\theta)_i$	$\ (\underline{H})_i\ $	$(\hat{\theta}_0)_i$	$\sqrt{(\underline{S}_0^\theta)_{ii}}$	$(\hat{\theta}_{100})_i$			$(\bar{\theta})_i$
				no noise	0.1% noise	1.0% noise	
E	0.4	0.8	0.04	1.0	1.001	1.010	1.0
ν	0.2	0.2	0.04	0.4	0.399	0.403	0.4
K_0	0.05	1.2	0.04	1.0	0.986	1.058	1.0
n_0	0.01	0.6	0.04	0.8	0.799	0.621	0.8

Table 3.2: Summary of estimation results using perfect observations and observations disturbed with two different noise levels.

of the noise is a percentage of respectively the maximum pressure, the maximum radial displacement and the maximum axial displacement on the interval $[0, 1]$. Both a 0.1% and a 1% noise level are studied.

3.4.4 Parameter estimation

Model errors do not occur, since exactly the same model is used for the identification as for the generation of ‘measurements’. To estimate the parameters, one iteration of the Newton-Raphson technique to solve (3.7) is executed. Consequently, equation (3.10) is solved once per time point. Initialisation of the algorithm requires an initial guess $\hat{\theta}_0$ for the parameters and an initial guess \underline{S}_0^θ for the parameter variance. The initial errors on the parameters are assumed to be mutually independent, so \underline{S}_0^θ is a diagonal matrix. The diagonal elements correspond with the square of the expected errors in the initial guess. To prevent that \underline{S}_r^θ becomes too small, at each time point a small positive definite matrix \underline{T} is added to \underline{S}_r^θ . During estimation \underline{T} is chosen to be equal to $0.01 \times \underline{S}_0^\theta$, which is rather arbitrary. In table 3.2, the values for $\hat{\theta}_0$, \underline{S}_0^θ , and the true values $\bar{\theta}$ of the parameters are given. The initial guess deviates from the true value with 20% for Young’s modulus to 50% for Poisson’s ratio. Also the maximum sensitivity during the analysis is given for each parameter. Here, $\|(\underline{H})_i\|$ denotes the maximum absolute value of the column of \underline{H} that corresponds to $(\theta)_i$.

The accuracy of the ‘measurements’ is taken into account via the variance matrix \underline{S}^m . As the errors on the distinct elements of the observations are mutually independent, \underline{S}^m is a diagonal matrix. For perfect observations the diagonal elements are set to 10^{-10} ; for observations disturbed with 0.1% noise and 1% noise, the diagonal elements are set to 10^{-8} and 10^{-6} respectively, which correspond with the square of the expected absolute errors on the observations.

The upper graph of Figure 3.5 shows the estimates of the model parameters as a function of time, starting with the initial guess $\hat{\theta}_0$, using perfect observations. The estimation procedure works well, since the estimates converge fast to their true values. The rate of convergence of E and ν is higher than the rate of convergence of K_0 and n_0 . It can be observed that a large rate of convergence of a parameter coincides with a large sensitivity of the output with respect to that parameter.

It may be difficult to determine the parameters if observations are disturbed by measurement errors. Figure 3.5 shows the estimation results using disturbed observations. The final estimates are summarised in table 3.2. In case of observations disturbed with 0.1% noise, it is possible to determine the four model parameters, although the rate of convergence has decreased. In contrast to Young's modulus and Poisson's ratio, the permeability and the porosity can not be determined accurately if observations are disturbed with 1% noise. These observations apparently do not offer sufficient information for the successful estimation of K_0 and n_0 .

In the left-hand column of Figure 3.6, the residuals between \hat{m}_i and \hat{y}_i during estimation are given for observations disturbed with 0.1% noise. These figures show that the algorithm gradually reduces the residuals to the noise level on the observations as the parameters converge. Until $t = 0.5$, the parameter estimates are adapted as the residuals are relatively large compared to the noise level. After $t = 0.5$, the parameters are only adapted slightly and the residuals no longer decrease.

Tests have also been performed with worse initial guesses for the parameters and different functions of time for the load. These tests showed the same phenomena as the test described above.

3.4.5 Influence of a model error

The estimation algorithm has been subjected to a second test, where a model error has been introduced as observations have been generated with a constitutive model different from the model used for estimation. The observations have been generated with a permeability that is given by (3.21). For the estimation, the permeability is assumed to be constant, i.e.

$$K = K_0. \quad (3.28)$$

Young's modulus, Poisson's ratio and the permeability are estimated, so $\theta = [E, \nu, K_0]^T$ and the porosity does not play any role in this model. The estimation algorithm is started with the same initial guesses for E , ν , and K_0 as in the first test and the same matrices \underline{S}_0^θ and \underline{T} are used. Since observations are not disturbed with measurement errors, the diagonal elements of \underline{S}^m are equal to 10^{-10} .

In Figure 3.7, the estimates are given as a function of time. Young's modulus and Poisson's ratio

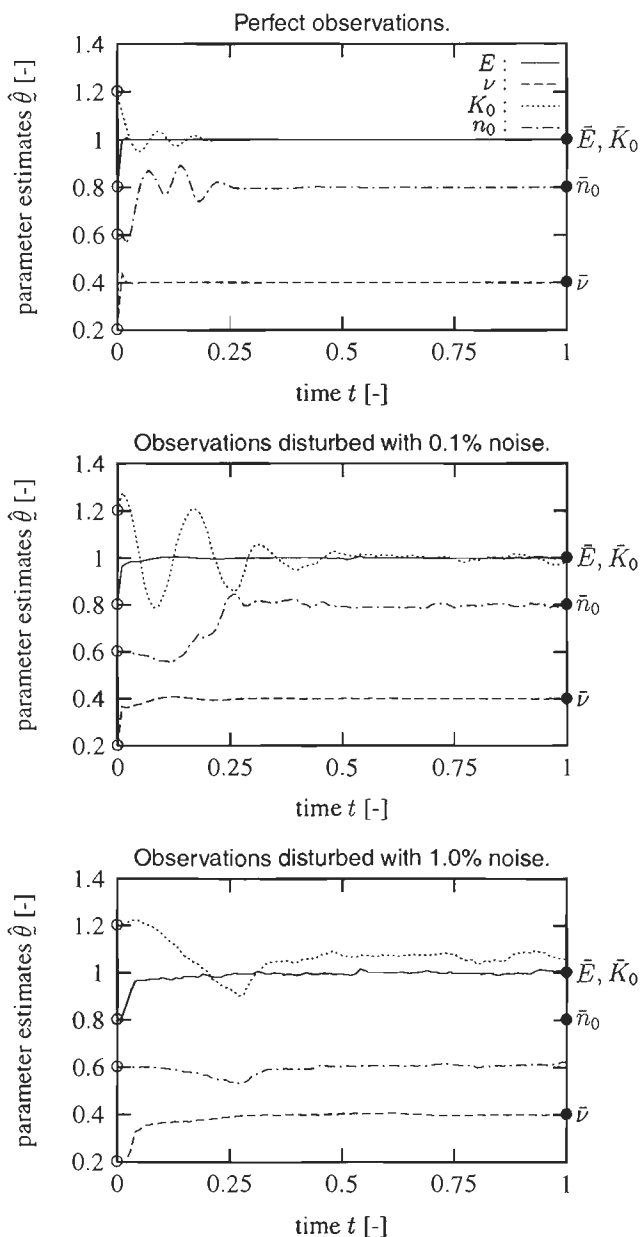


Figure 3.5: Parameter estimation in absence of model errors. The initial estimates are marked with \circ at $t = 0$, and the true values of the parameters are marked with \bullet at $t = 1$.

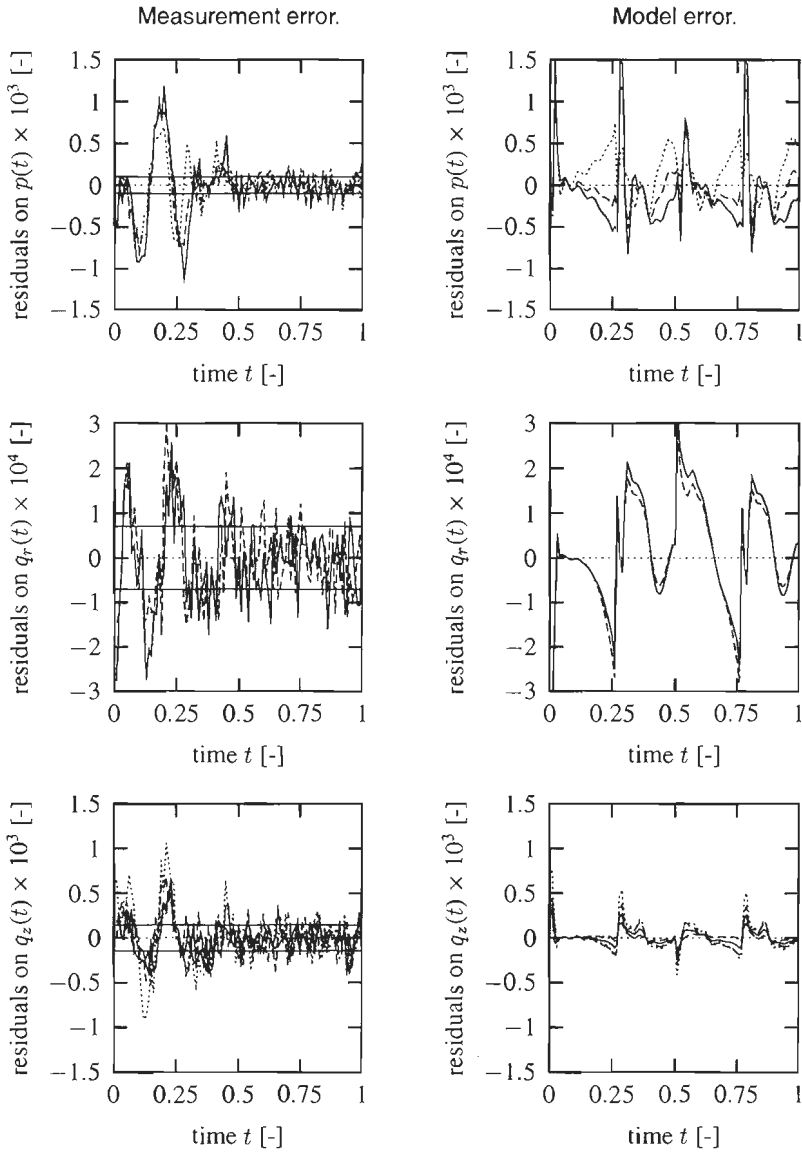


Figure 3.6: The residuals between 'measured' and computed pressures (upper row), radial displacements (center row) and axial displacements (lower row), during estimation. In the left-hand column, the residuals are given for estimation with 0.1% measurement error in absence of model errors (Section 3.4.4). The variance of the measurement error is shown by horizontal solid lines. In the right-hand column, residuals are given in case of a deliberate model error in the permeability (Section 3.4.5).

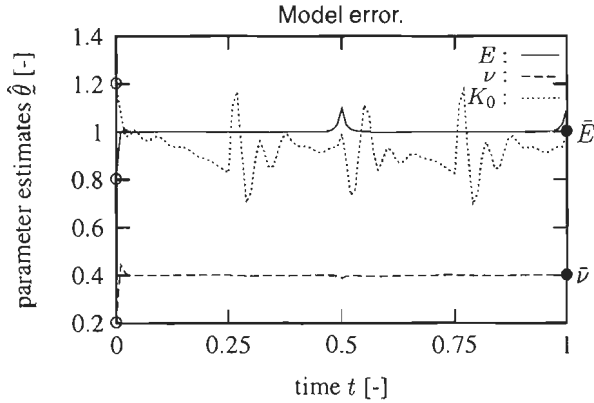


Figure 3.7: Parameter estimation in case of a model error in the permeability.

can be readily determined although deviations are observed if the load on the specimen is small ($t = 0.5, t = 1$). The algorithm determines a bounded value for K_0 , but K_0 does not converge due to the inhomogeneous deformation field in the specimen. Apparently, the algorithm locates the model error in the permeability, as E and ν are determined correctly. However, it is not possible to determine the type of model error in the permeability from Figure 3.7. In the right-hand column of Figure 3.6, the residuals between \underline{y}_i and \underline{m}_i are given. Due to the introduced model error, the residuals are periodic with the same period time as the force F . It can be observed that the residuals on the pressures are significantly larger than the residuals on the displacements. This suggests that pressures are related mainly to permeability, and displacements mainly to Young's modulus and Poisson's ratio.

3.5 Discussion

The tests in the previous sections have shown that it is possible to determine the parameters of a fluid-solid mixture with the recursive estimation algorithm. The influence of measurement errors and of a model error are studied. Up to a measurement error of 1%, the algorithm is able to estimate the parameters, although the rate of convergence of the parameters decreases with increasing error. Moreover, a model error with respect to the constitutive model for the permeability can be located with the algorithm. However, the adjustment of the model on the basis of estimation results requires additional research. It is noted that for a more general discussion on the possibilities of the algorithm, distinct model errors, e.g. in the constitutive model for the

solid, have to be investigated.

Due to the use of recursion and the pseudo-analytical method to determine the sensitivity, the method is very fast. A simulation –without estimation– over 100 time steps, with 144 elements, takes about 900 CPU-seconds on a Silicon Graphics Challenge R4400(150MHz)-processor. Estimation with the same number of time steps, and the same mesh, only requires about 300 seconds more. The total time required for estimation is of the same order as the time required for a single analysis.

As the standard identification technique in DIANA-PAREST is not fully recursive and because the sensitivity is determined numerically in this module, this technique would require a multiple of the computational time for one analysis. Application of the pseudo-analytical technique instead of numerical differentiation reduces the computational time by a factor $(N_\theta + 1)$, where N_θ is the number of model parameters (van Kemenade [1993]).

To determine the parameters, the nonlinear equation (3.7) is solved by a Newton-Raphson procedure. In the current implementation of the recursive algorithm however, only one iteration is performed. Therefore, the resulting estimates will deviate from the estimates determined by iterating until (3.7) has been satisfied exactly. To minimise this difference, the time interval between estimations has been restricted and estimates are determined at a large number of subsequent time points. If measurements are not available at small time intervals, it should be investigated whether the effect of performing only one iteration disturbs the estimation process. Consequently, the algorithm should be adapted to solve the parameter equations more accurately.

Chapter 4

An estimation algorithm with residuals on the model equations

4.1 Introduction

In the previous chapter the model parameters were determined by minimising the residuals between measurements and model output, while the model equations were satisfied exactly. However, after estimation the residuals may still be significant due to model errors. One of the objectives of identification is to improve on model errors on the basis of information from the identification procedure. To account for model errors, in this chapter it is not required that the model equations are satisfied exactly.

In Section 4.2 an *integral estimation algorithm* is presented (Veldpaus *et al.* [1996]). This algorithm accepts residuals on both the model and parameter equations. The model parameters and the displacement and pressure field are determined such that these residuals and the residuals between measurements and model output are minimised. For this purpose a scalar measure is set up by integrating the weighted squared residuals over the total experiment. Minimisation of this measure with respect to the parameters, the nodal displacements and the nodal pressures results in a set of differential and algebraic equations, which establishes a boundary value problem. This problem can be solved if the number of unknown nodal pressures is equal to the number of unknown nodal displacements.

In Section 4.3 the solution procedure is discussed for experiments satisfying this requirement. The resulting algorithm is elegant as it uses all measurements simultaneously. Therefore, the solution at each time point within the considered time interval is related to all measurements and it is a best fit in the sense that it minimises a measure of all residuals. Moreover, the algorithm provides much information via the residuals on the model equations, the parameter equation and the measurement equation, which is expected to be valuable for the detection of model errors.

The integral estimation algorithm is applied in Section 4.4 to simulations of a confined compression ‘experiment’. The influence of both ‘measurement’ and model errors on estimation is studied.

4.2 The integral estimation algorithm

As model errors not only result in residuals between measured and computed output but also in residuals on the model equations, an estimation algorithm which incorporates both kinds of error is elaborated. In this section the estimation procedure according to van de Molengraft [1990] is applied. This technique resembles the Extended Kalman Filtering (EKF) technique, which is based on the assumption that all errors are stochastic (Maybeck [1982]). However, in the case of material parameter identification, errors are due to, e.g., ill-modelled material behaviour and are mainly deterministic. Although the results of the approach presented in this chapter and of EKF are very much alike in a mathematical sense, the interpretation of the results is different.

The estimation procedure is based on an identification model consisting of the model equations (2.31) and (2.32), the parameter equations (2.38), and the output equations (2.60). It is assumed that for all $\tau \in [t_0, t_N]$ the input $\underline{u}(\tau)$ and a measured value $\underline{m}(\tau)$ of the output are available. The objective is to find for all $\tau \in [t_0, t_N]$ estimates $\hat{\underline{\theta}}(\tau)$ and corresponding estimates $\hat{\underline{q}}(\tau)$ and $\hat{\underline{p}}(\tau)$ such that the measured output $\underline{m}(\tau)$ corresponds best to the model output $\underline{y}(\tau)$ and that the model equations and the parameter equations are satisfied as good as possible. If residuals $\underline{\xi}$ and $\underline{\zeta}$ are accepted on these equations

$$\underline{\xi}_1(t) = \underline{B} \hat{\underline{q}} + \underline{K} \hat{\underline{p}} - \underline{s}, \quad (4.1)$$

$$\underline{\xi}_2(t) = \underline{f} - \underline{B}^T \hat{\underline{p}} - \underline{t}, \quad (4.2)$$

$$\underline{\xi}_3(t) = \dot{\hat{\underline{\theta}}}, \quad (4.3)$$

$$\underline{\zeta}(t) = \underline{m} - \underline{g}(\hat{\underline{q}}, \hat{\underline{p}}, \underline{u}), \quad (4.4)$$

then the objective is to find estimates $\hat{\underline{\theta}}$, $\hat{\underline{q}}$ and $\hat{\underline{p}}$ for which these residuals are minimal in the sense of the scalar measure

$$J = \int_{t_0}^{t_N} \left\{ \frac{1}{2} \sum_1^3 \underline{\xi}_i^T \underline{W}_i \underline{\xi}_i + \frac{1}{2} \underline{\zeta}^T \underline{V} \underline{\zeta} \right\} d\tau. \quad (4.5)$$

A time integral has been used since the residuals are functions on the interval $[t_0, t_N]$. The constant, symmetric, positive definite matrices \underline{W}_1 , \underline{W}_2 and \underline{W}_3 express confidence in the model and parameter equations while the constant, symmetric, (semi-) positive definite matrix \underline{V} is a

measure for the confidence in the measurements. Usually the weighting matrices are chosen diagonal, since it is difficult to choose reasonable values for the non-diagonal components.

A necessary, but not sufficient, condition for J to be minimal is that the variation δJ of J equals zero for all variations of $\hat{\theta}$, \hat{q} and \hat{p} .

The identification model (4.1) to (4.4) consists of algebraic and differential equations. The differential equations (4.1) and (4.3) are treated as constraints and are incorporated in an augmented measure J^* using Lagrange multipliers λ and μ

$$J^* = \int_{t_0}^{t_N} \left\{ \frac{1}{2} \sum_{i=1}^3 \xi_i^T \underline{W}_i \xi_i + \frac{1}{2} \underline{\zeta}^T \underline{V} \underline{\zeta} + \lambda^T [\underline{B} \hat{q} + \underline{K} \hat{p} - \underline{s} - \xi_1] + \mu^T [\hat{\theta} - \xi_3] \right\} d\tau. \quad (4.6)$$

Then, it is allowed to consider ξ_1 , ξ_3 , λ and μ as additional independent variables. This facilitates further elaboration. The requirement that $\delta J^* = 0$ for all variations of λ , μ , \hat{q} , $\hat{\theta}$, \hat{p} , ξ_1 , and ξ_3 leads to (Appendix C):

1. A set of differential equations

$$\underline{B} \hat{q} = \underline{W}_1^{-1} \lambda - \underline{K} \hat{p} + \underline{s}, \quad (4.7)$$

$$\hat{\theta} = \underline{W}_3^{-1} \mu, \quad (4.8)$$

$$(\underline{B}^T \lambda + \underline{B}^T \dot{\lambda}) = (\underline{L}^{sq})^T \lambda + (\underline{L}^{tq})^T \underline{W}_2 (f - \underline{B}^T \hat{p} - t) - (\underline{G}^q)^T \underline{V} (m - g), \quad (4.9)$$

$$\dot{\mu} = (\underline{L}^{s\theta})^T \lambda + (\underline{L}^{t\theta})^T \underline{W}_2 (f - \underline{B}^T \hat{p} - t), \quad (4.10)$$

with boundary conditions

$$\underline{B}^T \lambda(t_0) = \underline{0}, \quad \underline{B}^T \lambda(t_N) = \underline{0}, \quad (4.11)$$

$$\underline{\mu}(t_0) = \underline{0}, \quad \underline{\mu}(t_N) = \underline{0}. \quad (4.12)$$

2. A set of algebraic equations

$$\underline{K}^T \lambda - \underline{B} \underline{W}_2 (f - \underline{B}^T \hat{p} - t) - (\underline{G}^p)^T \underline{V} (m - g) = \underline{0}. \quad (4.13)$$

3. A relation between the residuals ξ_1 and ξ_3 , and the Lagrange multipliers λ and μ

$$\xi_1 = \underline{W}_1^{-1} \lambda, \quad (4.14)$$

$$\xi_3 = \underline{W}_3^{-1} \mu, \quad (4.15)$$

where $\underline{L}^{\alpha\beta}$ ($\alpha \in \{s, t\}$ and $\beta \in \{q, \theta\}$) are given by (2.46), (2.47), (2.56), and (2.57) while \underline{G}^q and \underline{G}^p are given by (2.62). The given set of equations establishes a two-point boundary value problem, since initial and end conditions are given for $\underline{B}^T \lambda$ and $\underline{\mu}$.

For a number of reasons, this set of equations is difficult to solve. Firstly, due to the nature of the problem, no initial conditions $\hat{\theta}(t_0)$ and $q(t_0)$ are available, but only initial guesses $\hat{\theta}_0(t)$ and $\hat{q}_0(t)$

for $t \in [t_0, t_N]$. The identification algorithm determines estimates of the initial conditions for q and θ such that the boundary conditions (4.11) and (4.12) are satisfied. Consequently, specific techniques for solving nonlinear boundary value problems have to be used (Ascher *et al.* [1988]). Secondly, in general the number of unknown nodal pressures n_p is smaller than the number of unknown nodal displacements n_q , so \underline{B} is not square as the dimension of \underline{B} is $n_p \times n_q$. Consequently, it is not possible to solve $\hat{\theta}(t)$, $\hat{q}(t)$ and $\hat{p}(t)$ by integrating (4.7) to (4.10) from t_0 to t , given (4.13). The reason for this is that λ shows up in (4.7), (4.10) and (4.13), while only a differential equation in $\underline{B}^T \lambda$ is available and \underline{B} is not invertible.

4.3 Solving the boundary value problem

To show the possibilities of the integral estimation algorithm, a simplified problem will be elaborated for which finite element modelling, taking the boundary conditions into account, results in a square and regular matrix \underline{B} . Then, the discretised balance equations of mass (2.31) can be rewritten as

$$\dot{q} = \underline{B}^{-1} (\underline{s} - \underline{K}p), \quad (4.16)$$

and the nodal pressures p are eliminated, using the discretised balance equations of momentum (2.32), i.e.

$$p = \underline{B}^{-T} (f - \underline{t}). \quad (4.17)$$

The differential equation (4.16) for q and the parameter equations $\dot{\theta} = \underline{Q}$ can be combined to yield

$$\dot{\underline{x}} = \underline{z}(\underline{x}, \underline{u}), \quad (4.18)$$

where

$$\underline{x} = \begin{bmatrix} q \\ \theta \end{bmatrix}, \quad \underline{z} = \begin{bmatrix} \underline{B}^{-1} (\underline{s} - \underline{K}p) \\ \underline{Q} \end{bmatrix}. \quad (4.19)$$

The column \underline{x} is called the state or, to emphasise that the unknown parameters are part of \underline{x} , the *extended state*. The measurement equation becomes

$$\underline{m} = \underline{g}(\underline{x}, \underline{u}). \quad (4.20)$$

The components of \underline{z} and \underline{g} are smooth functions of their arguments. The variations of \underline{z} and \underline{g} due to a variation $\delta \underline{x}$ are written as

$$\delta \underline{z} = \underline{Z} \delta \underline{x}, \quad \delta \underline{g} = \underline{G} \delta \underline{x}, \quad (4.21)$$

where

$$Z_{ij}(x, u) = \frac{\partial z_i}{\partial x_j}, \quad G_{ij}(x, u) = \frac{\partial g_i}{\partial x_j}. \quad (4.22)$$

The residuals on (4.18) and (4.20) are denoted by ξ and ζ

$$\xi = \hat{x} - z(\hat{x}, u), \quad (4.23)$$

$$\zeta = \underline{m} - \underline{g}(\hat{x}, u). \quad (4.24)$$

Due to elimination of p , no separate residuals on the balance equations of mass and the balance equations of momentum are distinguished. Minimisation of a scalar measure of ξ and ζ similar to (4.5) leads to a set of coupled differential equations

$$\dot{\hat{x}} = z + W^{-1} \lambda, \quad (4.25)$$

$$\dot{\lambda} = -Z^T \lambda - G^T V (\underline{m} - \underline{g}), \quad (4.26)$$

with boundary conditions for the *co-state* λ

$$\lambda(t_0) = \underline{0}, \quad \lambda(t_N) = \underline{0}. \quad (4.27)$$

Herein, W and V are weighting matrices for the errors ξ on the model equations and ζ on the measurement equations respectively. It is remarked that $W^{-1} \lambda = \xi$. These equations establish a boundary value problem since no initial condition for \hat{x} is available. To determine the solution for \hat{x} of this two point boundary value problem, various solvers are proposed, such as the multiple shooting algorithm and the collocation algorithm (Ascher *et al.* [1988]). Here, an approximating linearisation method will be used to decouple the differential equations for \hat{x} and λ . This method is based on the mathematical transformation

$$\hat{x} = \omega + \underline{\Omega} \lambda, \quad (4.28)$$

and on the observation that, for a perfect model without measurement errors, both $\xi(t) = W^{-1} \lambda(t)$ and $\zeta(t)$ are zero for all $t \in [t_0, t_N]$. Hence, for a reasonable model with moderate measurement errors it seems to be acceptable to assume that $\lambda(t)$ and $\zeta(t)$ are small. The variable ω denotes the state in the case that no model errors occur. In principle, the choice of the transformation matrix $\underline{\Omega}$ is still free.

The time derivative of \hat{x} becomes

$$\dot{\hat{x}} = \dot{\omega} + \dot{\underline{\Omega}} \lambda + \underline{\Omega} \dot{\lambda}. \quad (4.29)$$

Substitution of (4.28) and (4.29) into (4.25) and (4.26) results in a set of equations that is nonlinear in ω and λ . These equations can be solved iteratively. Therefore, the terms in these equations

are linearised around ω . If second and higher order terms in $\underline{\Omega}\lambda$ and products of $\underline{\Omega}\lambda$ and ζ are neglected, it follows that the equations for ω decouple from the equations for λ if the transformation matrix $\underline{\Omega}$ satisfies (Appendix D)

$$\dot{\underline{\Omega}} = \underline{W}^{-1} + \underline{\Omega} \underline{Z}^T(\omega, \underline{y}) + \underline{Z}(\omega, \underline{y}) \underline{\Omega} - \underline{\Omega} \underline{G}^T(\omega, \underline{y}) \underline{V} \underline{G}(\omega, \underline{y}) \underline{\Omega}. \quad (4.30)$$

Then, the resulting equations for ω and λ are given by

$$\dot{\omega} = z(\omega, \underline{y}) + \underline{\Omega} \underline{G}^T(\omega, \underline{y}) \underline{V} \left(\underline{m} - \underline{g}(\omega, \underline{y}) \right), \quad (4.31)$$

$$\dot{\lambda} = \left(\underline{G}^T(\omega, \underline{y}) \underline{V} \underline{G}(\omega, \underline{y}) \underline{\Omega} - \underline{Z}^T(\omega, \underline{y}) \right) \lambda - \underline{G}^T(\omega, \underline{y}) \underline{V} \left(\underline{m} - \underline{g}(\omega, \underline{y}) \right). \quad (4.32)$$

The value of ω at time t_0 is unknown a priori. With any guess $\omega(t_0)$ for this initial value and a chosen $\underline{\Omega}(t_0)$, the equations (4.30) and (4.31) can be solved simultaneously by forward integration. After that, equation (4.32) can be solved by backward integration, using the end condition $\lambda(t_N) = \underline{0}$. In general, the obtained solution for $\lambda(t)$ will not satisfy the initial condition $\lambda(t_0) = \underline{0}$. The solution $\lambda(t_0)$ depends on the input $\underline{y}(\tau)$ and the measurements $\underline{m}(\tau)$ for $\tau \in [t_0, t_N]$ and on $\omega(t_0)$. Hence, the problem is to determine $\omega(t_0)$ such that $\lambda(t_0) = \underline{0}$. A simple iterative algorithm is used to solve this problem. It is assumed that a ‘reasonable’ estimate \hat{x}_0 for the initial state is known. With $\omega(t_0) = \hat{x}_0$ the solutions for ω , $\underline{\Omega}$ and λ are calculated and $\hat{x}(t_0)$ is determined from $\hat{x}(t_0) = \underline{\Omega}(t_0)\lambda(t_0) + \omega(t_0)$. If some measure, e.g. the length of $\lambda(t_0)$, is larger than a predefined tolerance, then the next step in the iteration is taken, starting with $\hat{x}(t_0)$ as the initial value $\omega(t_0)$. If the measure is smaller than the tolerance, then the iteration is stopped and the state $\underline{x}(\tau)$ is calculated for $\tau \in [t_0, t_N]$, using $\underline{x}(\tau) = \underline{\Omega}(\tau)\lambda(\tau) + \omega(\tau)$. At the moment no proof of the convergence of this iterative algorithm is available and it remains to be investigated whether or not this method is to be preferred to more conventional shooting methods.

4.4 Testing of the integral algorithm

A simulation study is performed and the integral estimation method is used to determine the unknown parameters from the simulated confined compression test. Since finite element modelling of this ‘experiment’ results in a regular matrix \underline{B} , the estimation procedure proposed in the previous section can be applied.

4.4.1 ‘Experimental’ set-up

In the confined compression test, a specimen of a fluid-solid mixture is placed in a rigid, impermeable, cylindrical container (radius $R_0 = 1$) with a rigid, impermeable bottom and a rigid

piston at the top (Figure 4.1). In the unloaded configuration \mathcal{B}_0 at time $t_0 = 0$, the specimen is homogeneous with height $H_0 = 1$.

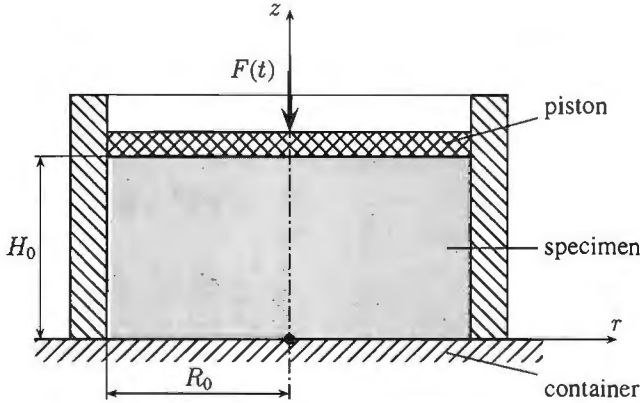


Figure 4.1: 'Experimental' set-up.

Radial displacements at the cylindrical part of the container and axial displacements of the mixture particles at the bottom are suppressed, so

$$q_r(r_0, z_0, t) = 0, \quad q_z(r_0, z_0 = 0, t) = 0. \tag{4.33}$$

The piston behaves as a sieve for the fluid but is impermeable for the solid. Therefore, it is assumed that the pressure at the piston is equal to zero

$$p(r_0, z_0 = H_0, t) = 0. \tag{4.34}$$

For $t \geq 0$ the specimen is loaded by an axial force $F(t)$ on the piston. This force is seen as the input of the 'experiment'. The axial displacement $q_z(H_0, t)$ of the solid at the top equals the displacement of the piston. The load on the piston causes deformation of the solid and squeezes fluid through the piston out of the mixture. Friction between piston, container and mixture is neglected, so there are no shear stresses at the boundaries of the specimen. Guided by the boundary conditions and by the rotational symmetry of the specimen, it is assumed that the mixture particles only move in axial direction. Therefore, a one-dimensional problem results and \bar{q} and p only depend on the axial coordinate z and on time t but not on the radial or the circumferential coordinate.

The measured quantities are the axial displacement of the piston and the pressure at the bottom of the container at 200 equally distributed time points in the interval $[0, 1]$.

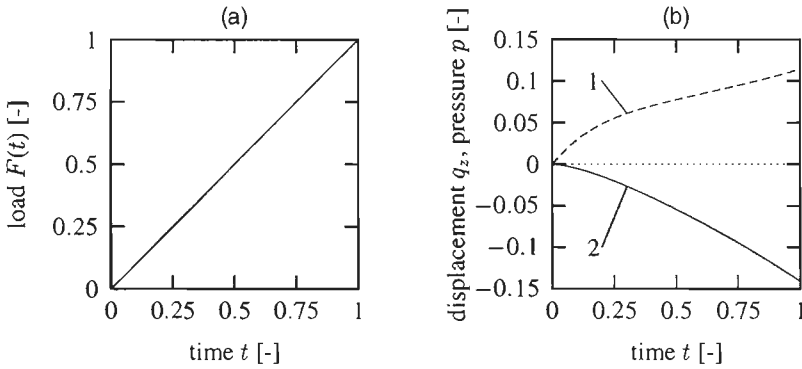


Figure 4.2: Analysis of the confined compression 'experiment': (a) the applied compressive load versus time; (b) the pressure $p(t)$ at the bottom (1) and the axial displacement $q_z(t)$ of the piston (2).

4.4.2 Finite element analysis

The constitutive model for the generation of 'measurement' data is discussed in Section 3.4.1. The true parameter set $\bar{\theta}$ is equal to

$$\bar{\theta} = [1.0, 0.4, 1.0, 0.8]^T. \quad (4.35)$$

The specimen is modelled by 16 elements of equal length $H_0/16$. The nodal displacements at the bottom are suppressed. Since the piston behaves as a sieve, the nodal pressures at the top are equal to zero for all t . Figure 4.2(a) depicts the applied load $F(t)$ as a function of time from $t = 0$ to $t = 1$. With a maximum load $F = 1$, a maximum Green-Lagrange strain of about 0.2 is achieved.

The computed displacement of the piston and the pressure at the bottom of the container are given in Figure 4.2(b). To study the influence of measurement errors, the analysis results are disturbed by noise with a zero mean normal distribution. The standard deviation of the noise is equal to 1% of respectively the maximum pressure and the maximum displacement occurring on the interval $[0, 1]$.

4.4.3 Parameter estimation

Firstly, the method is tested by estimating the parameters from analysis results that are disturbed by 1% noise. In this first test the identification model equals the simulation model, i.e. there are no model errors. In a confined compression test, the measurements are not sufficient to determine both E and ν . However, they are rich enough to determine the confined compression modulus C

which is defined as

$$C = \frac{E(1-\nu)}{(1+\nu)(1-2\nu)}, \quad \bar{C} = 2.143, \quad (4.36)$$

where \bar{C} is the true confined compression modulus with $\bar{E} = 1.0$ and $\bar{\nu} = 0.4$. As a consequence, the column of unknown, constant parameters reduces to $\theta = [C, K_0, n_0]^T$.

The first 16 components of the extended state \underline{x} are the unknown nodal displacements. The components 17, 18 and 19 are the model parameters. The weighting matrix \underline{W} for the residuals on the model and parameter equations (4.25) and the weighting matrix \underline{V} for the residuals on the output equations (4.26) are chosen diagonal with

$$\underline{W} = \text{diag}(1, \dots, 1, W_{17}, W_{18}, W_{19}), \quad \underline{V} = \text{diag}(1, 1), \quad (4.37)$$

where, for the moment, $W_{17} = W_{18} = W_{19} = 1$. This means that all extended state equations are equally trusted.

The diagonal initial value $\underline{\Omega}(t_0)$ for the symmetric transformation matrix $\underline{\Omega}$ and the first guess ω_0 for the initial condition $\omega(t_0)$ are chosen as

$$\underline{\Omega}(t_0) = \text{diag}(0, \dots, 0, 10^5, 10^5, 10^5), \quad (4.38)$$

$$\omega_0 = (0, \dots, 0, 3, 3, 1)^T, \quad (4.39)$$

where $\omega_0^T = [\hat{q}_0^T, \hat{\theta}_0^T]$. In analogy with the EKF-theory, $\underline{\Omega}(t)$ can be interpreted as a measure of the uncertainty of the state estimate $\hat{x}(t)$. According to (4.28), $\underline{\Omega}(t)\lambda(t)$ is equal to the difference between $\hat{x}(t)$ and $\omega(t)$. If the components of the diagonal of $\underline{\Omega}(t)$ are large, then the corresponding components of $\hat{x}(t)$ are allowed to deviate much from the components of $\omega(t)$. Consequently, the components of the diagonal of $\underline{\Omega}(t_0)$ are a measure for the confidence in the initial state estimate $\omega(t_0) = \hat{x}(t_0)$. The components of $\underline{\Omega}(t_0)$ that weight the initial parameter estimates are chosen large to express that these estimates may be very bad. The initial conditions for the nodal displacements are assumed to be known exactly.

The estimation results are shown in Figure 4.3. The estimator provides the best possible constant parameter estimates within 5 iterations. Although 1% noise is added to the observations, the estimator is able to determine the correct values for the parameters. The estimator reduces the residuals between the 'measurements' and the estimated position and pressure to the level of the noise on the observations over the total interval. In contrast to Figure 3.5, this figure does not show the convergence behaviour of the estimates as the integral algorithm determines per iteration the time-dependent estimates over the total interval. The results are summarised in Table 4.1.

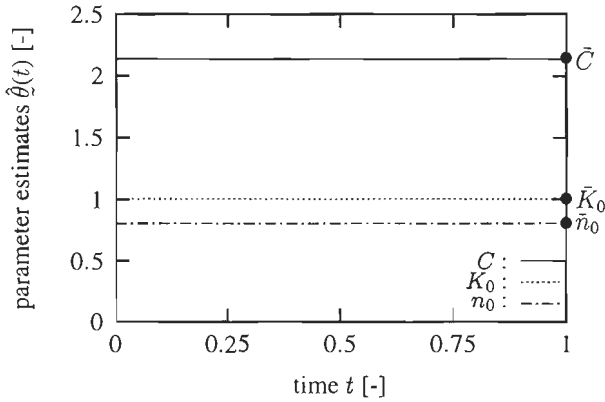


Figure 4.3: Parameter estimation in absence of model errors, while observations are disturbed with 1% noise. The initial estimates are $\hat{C} = 3$, $\hat{K}_0 = 3$, and $\hat{n}_0 = 1$. The true values of the parameters are marked with \bullet at $t = 1.0$.

Parameters $(\theta)_i$	Initial guess $(\hat{\theta}_0(t_0))_i$	Estimation results $(\hat{\theta})_i$		true value $(\bar{\theta})_i$
		1% measurement error	model error	
C	3.0	2.137	2.170	2.143
K_0	3.0	1.004	0.814	1.0
n_0	1.0	0.802	n.e.	0.8

Table 4.1: Summary of estimation results. The porosity n_0 is not estimated (n.e.) when the permeability in the identification model is deformation independent.

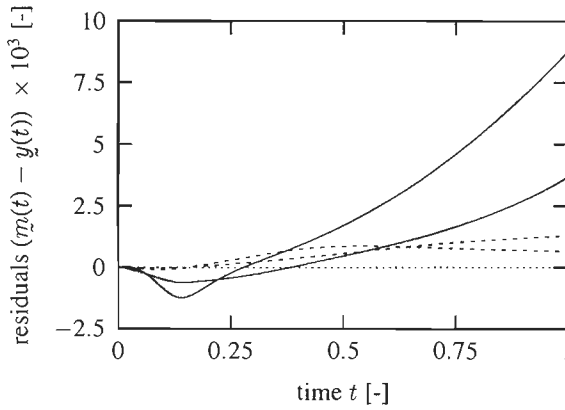


Figure 4.4: The residuals between measured and estimated position and pressure versus time in case of constant material parameters (solid lines) and in case of time-varying parameters (dashed lines).

4.4.4 Influence of a model error

For the second test, the deformation dependency of the permeability is not included in the identification model and the permeability is assumed to be constant (3.28). In this case the observations, that are generated with the deformation dependent model for the permeability (3.1), are not disturbed with noise. Two parameters are estimated, i.e. the confined compression modulus C and the permeability K_0 , so $\theta = [C, K_0]^T$. The weighting matrices \underline{W} , \underline{V} and $\underline{Q}(t_0)$, and the initial state estimate ω_0 remain unchanged, except for the last component of ω_0 and of the diagonals of \underline{W} and \underline{Q} . This component is omitted, as the porosity n_0 is no longer part of the identification model.

The estimator yields constant parameter estimates $\hat{C}(t) = 2.170$ and $\hat{K}_0(t) = 0.814$. This is achieved by choosing the components W_{17} and W_{18} , that weight the residuals on the parameter equations, equal to 1. Then, the parameter equations are strictly satisfied. Figure 4.4 (solid lines) shows significant residuals between $m(t)$ and $y(t)$, which indicates the presence of a model error. It is possible to locate this error by repeating the estimation procedure with weighting factors $W_{17} = W_{18} = 10^{-5}$, i.e. relaxing the parameter equations. If only one parameter estimate becomes time-varying, the error results from either permeability-related phenomena or stiffness-related phenomena in the model.

In Figure 4.5, the resulting parameter estimates are shown as a function of time. The estimated confined compression modulus \hat{C} is nearly constant, while the permeability estimate \hat{K}_0 clearly shows time-dependent behaviour. If the latter is compared to the deformation dependent permeability of the elements at the container bottom surface and the piston respectively, that is

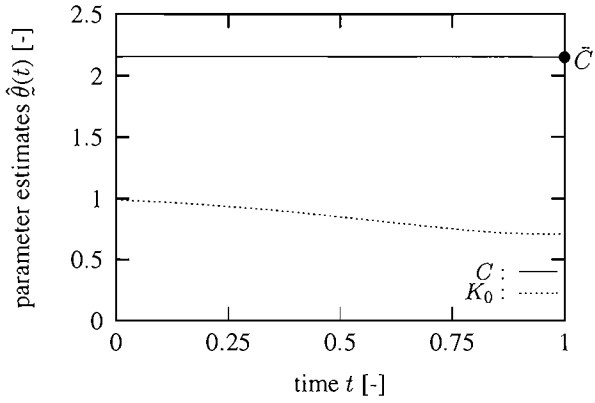


Figure 4.5: Parameter estimation in case of a model error in the permeability.

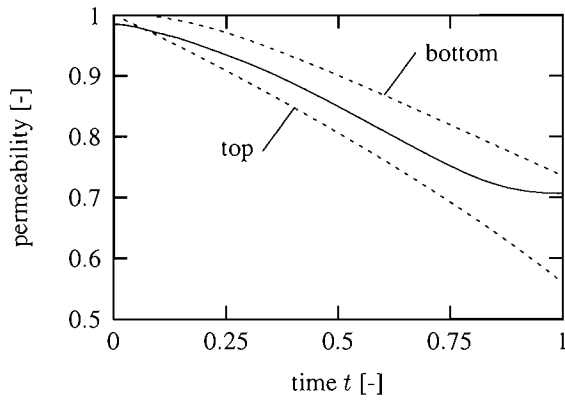


Figure 4.6: Estimated (solid) and actual (dashed) permeability versus time.

calculated according to the permeability model used to generate observations, then it appears that the estimate is a good compromise between them (Figure 4.6). The residuals on the measurement equations decrease significantly by allowing the parameters to vary with time (Figure 4.4, dashed lines). The estimator located the model error in the permeability and adjusted the estimate correctly.

4.5 Discussion

The integral estimation method yields good results for a simulation study on a confined compression test. When observations are disturbed with 1% noise, the algorithm is able to determine the correct material parameters. An important feature of the method is its potential to locate a model error in the permeability. It is even possible to detect how to improve the model by comparing the load on the specimen with the time-varying permeability. However, it must be noted that in a practical situation, it will be far more difficult to recognise various simultaneously occurring model errors in a quantitative sense.

The method is fast in case of a confined compression experiment, since the model equations are programmed directly in FORTRAN-code. A simulation with the model over 200 time steps, with 16 elements, takes less than one CPU-second on a PC 486-DX2(66MHz) processor. One iteration during estimation requires about 300 CPU-seconds. However, the computational time depends at least quadratically on the number N_x of state variables, as the number of ordinary differential equations to be solved is equal to $2N_x$ (for the components of the extended state) plus N_x^2 (for the components of \underline{Q}). Due to the simplicity of the confined compression experiment, the number of state variables is limited. For more complex problems computational time is expected to increase considerably.

Still some issues have to be investigated. Firstly, the numerical solution procedure of the two point boundary value problem has to be studied to gain insight into efficiency, numerical stability and convergence. Secondly, the matrix \underline{B} is in general not invertible. The model equations consist of a set of first-order differential equations in the unknown nodal displacements and a set of algebraic equations. Possibly, the column of unknown nodal displacements can be transformed in order to reduce the number of differentiated displacement variables to the number of unknown nodal pressures n_p . As a result, n_p algebraic equations will be added to the initial set of model equations. These equations will express the displacement variables to be differentiated in terms of the unknown nodal displacements. If the matrix \underline{B} is *no* function of the nodal displacements, this transformation will be very straightforward. Additional research is required to deal with this problem.

Chapter 5

Discussion, conclusions and recommendations

5.1 Discussion

To identify the parameters in constitutive models for complex material behaviour, numerical-experimental techniques have been developed. The parameters are determined by comparing measured field quantities with the outcome of numerical analyses of experiments. Therefore, an estimation algorithm is required which adjusts the values of the parameters so that the difference between measured and calculated field quantities is minimised. As a result of the large amount of information in the measured field quantities material parameters can be determined, even in situations where standard techniques fail.

The objective of the research presented in this thesis was to study estimation algorithms for application to materials with time-dependent behaviour. A fully recursive and an integral estimation algorithm were discussed. These algorithms were applied to a material, described by a two component fluid-solid mixture model where the interaction between the fluid and the solid component gives rise to visco-elastic behaviour. The differential and algebraic model equations are nonlinear in the displacements and the parameters and linear in the pressures. Information on time-dependent mixture behaviour was obtained by subjecting a specimen of mixture material to a time-dependent load while displacements and pressures were ‘measured’.

To test the algorithms, simulations of experiments were performed. The parameters were estimated from observation data that were generated by adding noise to the outcome of the simulations. Moreover, the influence of a single model error on the results of the algorithms was investigated. The model parameters consisted of Young’s modulus, Poisson’s ration, the initial permeability and the initial porosity of the solid. The porosity appears in the model to calculate the deformation dependent permeability.

Firstly, a recursive algorithm has been presented. Measurements at subsequent time points t_i are sequentially used by the algorithm. Starting from an initial guess for the parameters at $t = t_0$, the

algorithm yields estimates $\hat{\theta}_i$ of the parameters on the basis of the difference between the measured output and the computed model output at time point t_i . Information from measurements on previous time points is taken into account by incorporating the previous parameter estimate $\hat{\theta}_{i-1}$. To compute the model output at t_i , given this estimate of the parameters, the model equations are solved over the interval $[t_{i-1}, t_i]$ only. Weighting matrices are used to balance between the confidence in the measurements m_i and the confidence in the previous estimate $\hat{\theta}_{i-1}$. The algorithm also requires the sensitivity matrix which is the derivative of the model output with respect to the parameters. This matrix is computed by a pseudo-analytical method.

Secondly, an integral estimation procedure, which uses the measurements in all measurement time points simultaneously, has been studied. In this algorithm (in contrast to the previous) it is not assumed that the model and the parameter equations are satisfied exactly. Therefore, it accepts residuals on these equations. The parameters, the displacements and the pressures are estimated simultaneously over the total time interval. For that purpose, the integral over this interval of a scalar measure of the residuals on the model equations, the residuals on the parameter equation and the residual between observations and the model output has to be minimised, which leads to a two point boundary value problem. This algorithm yields a smoothed solution for the parameters, the displacement field and the pressure field. By specification of weighting matrices, the user is able to determine to what extent the model equations, the parameter equation and the measurement equation are satisfied.

Both the recursive and the integral algorithm can be used to determine the model parameters of a fluid-solid mixture. The recursive algorithm is very efficient as a result of the pseudo-analytical method to determine the sensitivity matrix as specified in Chapter 2 and the recursive approach. The required computational time for the identification process, using all measurements over the experiment time interval, is of the same order as the time required for a single simulation over this interval.

The integral algorithm involves much more computational effort than the recursive algorithm. For a simple problem, such as the confined compression experiment, the required computational time is limited. However, for more complex problems, the computational time will increase considerably due to stability problems while solving the boundary value problem. At the moment, in case of fluid-solid mixtures, the integral algorithm can only be used if spatial discretisation of the model equations results in an equal number of unknown nodal displacements and unknown nodal pressures ($n_q = n_p$). The considered confined compression test is such an experiment. Only then, the inverse of the matrix \underline{B} in the model equation (4.1) can be computed to solve the boundary value problem (4.7) to (4.15). It has to be investigated yet how the boundary value problem can

be solved if the number of unknown nodal displacements is not equal to the number of unknown nodal pressures ($n_q \neq n_p$).

If the residuals between model output (determined with the estimated parameters) and measurements are not satisfactory, then, either the experiment does not provide sufficient information on the material behaviour, or the constitutive model is not able to describe the material behaviour sufficiently accurate. To prevent the first cause, simulations of experiments can be performed in advance. An important tool in these studies is the sensitivity matrix. A small sensitivity of the model output for a parameter indicates that the measurements will contain little information with respect to this parameter and that an adaptation of the experiment (geometry, boundary or loading conditions) is required. If unsuccessful identification is due to shortcomings in the constitutive model, then one would like to acquire indications for model improvements from the identification results. For this purpose, the residuals between measured and computed output after estimation of the parameters may be used. Experience and knowledge from previous experiments may yield suggestions for model corrections and the sensitivity matrix may be used to determine the influence of these corrections on the residuals in order to make a selection.

The estimation algorithms presented in this thesis provide additional information. The recursive and the integral method yield the model parameters as a function of time, but the behaviour of the parameters in time differs for the distinct methods. This is a result of the different measures that are minimised for the determination of the parameters. The algorithms also provide values for the residuals between measured and computed output and for the residuals on the model equations. For the recursive method, the latter can be determined by substitution of the final set of parameters, the solutions of the displacements and pressures and the input into the model equations.

It is expected that this information can be used to detect model errors, but it has to be investigated yet how to use the information for this purpose. For two simple problems, i.e. a confined and a bulge compression test, the influence of a single model error on the model parameters versus time has been studied. For that purpose, observations were generated with a deformation dependent permeability, while for identification a model with a constant, deformation independent permeability was used. Consequently, the porosity was no longer part of the constitutive model. If during identification the parameter equation was lightly weighted compared to the measurement equation, which means that the confidence in the measurements is much greater than the confidence in the parameter estimate at the previous time point, both algorithms showed clearly time varying behaviour of the permeability parameter, while constant values were found for the other parameters (Young's modulus and Poisson's ratio). The algorithms located the model error in the permeability correctly. Consequently, it seems to be worthwhile to investigate how the

information originating from the identification procedure can be used in case of various simultaneously occurring model errors, with other materials and other constitutive models.

The derivation of the algorithms was focused on materials whose behaviour can be described by the model equations (2.31) and (2.32). Since these equations are given in a general state-space formulation and include elastic and time-dependent mixture behaviour, no severe problems are expected for the application of the estimation algorithms to other visco-elastic materials. This enlarges the field of application of the algorithms considerably. Application to fluids or materials showing elasto-plastic behaviour requires additional research. Elasto-plastic materials do not return to their initial configuration after unloading. Therefore, the influence of initial conditions at $t = t_i$, which contain errors since they are based on a parameter estimate $\hat{\theta}$, will not decrease with time as for visco-elastic materials. The consequences of such behaviour with respect to identification will also be subject of future investigations.

5.2 Conclusions

- The recursive and the integral estimation algorithm are able to determine the model parameters of a two-component fluid-solid mixture.
- The recursive estimation algorithm is very efficient, since the time required for identification using all measurements is of the same order as the time required for a single simulation over the experiment time interval.
- The integral algorithm is very time-consuming even for simple problems and, at the moment, can only be used in a situation where spatial discretisation of the model equations for an experiment results in an equal number of unknown nodal displacements and unknown nodal pressures.
- It is demonstrated that the recursive and the integral estimation algorithm offer new possibilities in the detection of model errors. Here, the influence of a model error in the description of the permeability has been studied. Both algorithms were able to locate this error correctly.
- The sensitivity matrix is important not only during identification, but also in the investigations on model errors and during the evaluation of experiments. The identifiability of the parameters can be studied by use of the sensitivity matrix. Therefore, it is advantageous that the sensitivity matrix can be determined very fast by means of the pseudo-analytical method. Determination with this method is approximately $(N_\theta + 1)$ times as fast as numerical determination, where N_θ is the number of model parameters.

5.3 Recommendations

- It has to be investigated how the information provided by the identification algorithms can be used for the detection of model errors. As a first step the influence of distinct, well-defined model errors on the outcome of the identification procedure should be studied by the use of simulations. This may lead to clues how to extract suggestions for model corrections from the provided information.
- During real experiments unknown model errors and measurement errors will occur simultaneously. Therefore, performing laboratory experiments is an essential step in the evaluation of the identification techniques. As measurement data have to contain sufficient information to determine all parameters, including those related to time-dependent behaviour, time-dependent loading should be applied in the experiments.
- If the integral estimation algorithm is used, a two point boundary value problem appears. To solve this problem without constraints on the number of nodal displacements and nodal pressures, the model equations have to be reformulated. However, the integral algorithm does not offer sufficient additional advantages in comparison to the recursive algorithm to counterbalance the problems that are expected to make this method practically applicable. Therefore, the recursive algorithm is preferred to the integral algorithm.
- Until now, the numerical-experimental technique has been used mainly for the identification of elastic materials. The present research demonstrated the suitability of this technique for the identification of materials described by a fluid-solid mixture model. It is expected that application to fluids or materials described by other visco-elastic models is also possible without large modifications. This is a result of the general formulation of the model equations. Application to materials showing elasto-plastic behaviour requires additional research.
- The technique described in this thesis is designed for biphasic fluid-solid mixtures. This offers challenging possibilities in biomechanics because mixtures are suitable to describe the material behaviour of biological tissues. An additional advantage is that there exist techniques to measure quantities inside tissues (CT, MRI, MRI with tagging). Therefore, it becomes possible to perform an in-vivo material characterisation. Since this requires three-dimensional modelling, the efficient recursive estimation algorithm will be indispensable.
- With respect to biomechanical applications, it is worthwhile to extend the algorithm to triphasic mixtures of a solid, a fluid, and charged particles.

Bibliography

- Anderson, B.D.O. and Moore, J.B. [1973]. *Optimal Filtering*. Prentice Hall, Englewood Cliffs, New Jersey.
- Ascher, U.M., Mattheij, R.M.M., and Russell, R.D. [1988]. *Numerical Solution of Boundary Value Problems for Ordinary Differential Equations*. Prentice Hall, Englewood Cliffs, New Jersey.
- Bathe, K.J. [1982]. *Finite Element Procedures in Engineering Analysis*. Prentice Hall, Englewood Cliffs, New Jersey.
- Biot, M.A. [1941]. General theory of three-dimensional consolidation. *J. Appl. Phys.*, 12, 155–164.
- de Borst, R., Kusters, G.M.A., Nauta, P., and de Witte, F.C. [1985]. DIANA - a comprehensive, but flexible finite element system. In C.A. Brebbia, editor, *Finite Element Systems; a handbook*. Springer Verlag, Berlin, New York, and Tokyo.
- Bovendeerd, P.H.M., Arts, T., Huyghe, J.M., van Campen, D.H., and Reneman, R.S. [1992]. Dependence of local left ventricular wall mechanics on myocardial fiber orientation: a model study. *J. Biomech.*, 25(10), 1129–1140.
- Bowen, R.M. [1976]. Theory of mixtures. In A.C. Eringen, editor, *Continuum Physics*. Academic Press, New York.
- Bowen, R.M. [1980]. Incompressible porous media models by use of the theory of mixtures. *Int. J. Engng. Sci.*, 18, 1129–1148.
- Breukink, C.J. [1994]. Design of a method for in-vivo, mechanical characterization of human skin. Technical report, IVO, Eindhoven University of Technology, Eindhoven, The Netherlands.
- Fung, Y.C. [1965]. *Foundations of Solid Mechanics*. Prentice Hall, Englewood Cliffs, New Jersey.
- Haug, E.J., Choi, K.K., and Komkov, V. [1986]. *Design Sensitivity Analysis of Structural Systems*. Academic Press, Orlando.
- Hendriks, M.A.N. [1991]. *Identification of the Mechanical Behaviour of Solid Materials*. Ph.D. thesis, Eindhoven University of Technology, Eindhoven, The Netherlands.

- Hou, J.S., Holmes, M.H., Lai, W.M., and Mow, V.C. [1989]. Boundary conditions at the cartilage-synovial fluid interface for joint lubrication and theoretical verification. *J. Biomech. Eng.*, 111, 78–87.
- Hsieh, C.C. and Arora, J.S. [1985]. Structural design sensitivity analysis with general boundary conditions: Dynamic problem. *Int. J. Num. Meth. in Eng.*, 21, 267–283.
- Hunter, S.C. [1983]. *Mechanics of Continuous Media*. Ellis Horwood, Chichester.
- Huyghe, J.M., Arts, T., van Campen, D.H., and Reneman, R.S. [1992]. Porous medium finite element model of the beating left ventricle. *Am. J. Physiol.*, 262, H1256–H1267.
- Huyghe, J.M.R. [1986]. *Non-Linear Finite Element Models of the Beating Left Ventricle and the Intramyocardial Coronary Circulation*. Ph.D. thesis, Eindhoven University of Technology, Eindhoven, The Netherlands.
- van Kemenade, P.M. [1993]. Identification of the mechanical behaviour of nonlinear elastic materials. Technical report, Eindhoven University of Technology (WFW-report 93.071), Eindhoven, The Netherlands.
- Kulkarni, M. and Noor, A.K. [1995]. Sensitivity analysis of the non-linear dynamic viscoplastic response of 2-D structures with respect to material parameters. *Int. J. for Num. Meth. in Eng.*, 38, 183–198.
- Lai, W.M. and Mow, V.C. [1980]. Drag induced compression of articular cartilage during a permeation experiment. *Biorheology*, 17, 111–123.
- Laible, J.P., Pfister, D., Simon, B.R., Krag, M.H., Pope, M., and Haugh, L.D. [1994]. A dynamic material parameter estimation procedure for soft tissue using a poroelastic finite element model. *J. Biomech. Eng.*, 116(1), 19–29.
- van Lankveld, M.A.M. [1994]. *The mechanical behavior of the tibiofemoral joint - a numerical study on material and geometric parameters-*. Ph.D. thesis, Eindhoven University of Technology, Eindhoven, The Netherlands.
- Luenberger, D.G. [1966]. Observers for multivariable systems. *IEEE Transactions on Automatic Control*, AC-11(2), 190–197.
- Maybeck, P.S. [1982]. *Stochastic Models, Estimation, and Control*, volume 2. Academic Press, New York and London.
- van de Molengraft, M.J.G. [1990]. *Identification of Non-Linear Mechanical Systems for Control Application*. Ph.D. thesis, Eindhoven University of Technology, Eindhoven, The Netherlands.
- Mow, V.C., Kuei, S.C., Lai, W.M., and Armstrong, C.G. [1980]. Biphasic creep and stress relaxation of articular cartilage in compression: Theory and experiments. *J. Biomech. Eng.*, 102, 73–84.
- Müller, I. [1968]. A thermodynamic theory of mixtures of fluids. *Arch. Rational Mech. Anal.*, 28, 1–39.

- Oomens, C.W.J., van Campen, D.H., and Grootenboer, H.J. [1987]. A mixture approach to the mechanics of skin. *J. Biomech.*, 20, 877–885.
- Oomens, C.W.J., van Ratingen, M.R., Janssen, J.D., Kok, J.J., and Hendriks, M.A.N. [1993]. A numerical–experimental method for a mechanical characterization of biological materials. *J. Biomech.*, 26, 617–621.
- Op den Camp, O.M.G.C., van Houten, J.G.A., Oomens, C.W.J., Veldpaus, F.E., Janssen, J.D., and Kok, J.J. [1994]. The estimation of material parameters of a fluid-solid mixture. In G.M.A. Kusters and M.A.N. Hendriks, editors, *DIANA Computational Mechanics '94*, pages 85–92, Kluwer, Delft, The Netherlands.
- van Ratingen, M.R. [1994]. *Mechanical Identification of Inhomogeneous Solids - A Mixed Numerical Experimental Approach* -. Ph.D. thesis, Eindhoven University of Technology, Eindhoven, The Netherlands.
- van Ratingen, M.R., Petterson, R., Drost, M.R., Oomens, C.W.J., and Janssen, J.D. [1993]. A numerical experimental method to find Langer's lines of skin. In *Proc. WAM ASME, New Orleans*.
- Saffman, P.G. [1971]. On the boundary conditions at the surface of a porous medium. *Studies in Applied Mathematics*, 50, 93–101.
- Schreppers, G.J.M.A. [1991]. *Force Transmission in the Tibio–Femoral Contact Complex*. Ph.D. thesis, Eindhoven University of Technology, Eindhoven, The Netherlands.
- Simon, B.R., Wu, J.S.S., Carlton, M.W., Evans, J.H., and Kazarian, L.E. [1985]. Structural models for human spinal motion segments based on a poroelastic view of the intervertebral disk. *J. Biomech. Eng.*, 107, 327–335.
- Snijders, J.M.A. [1994]. *The Triphasic Mechanics of the Intervertebral Disc -a Theoretical, Numerical and Experimental Analysis*-. Ph.D. thesis, University of Limburg, Maastricht, The Netherlands.
- Spilker, R.L., Suh, J.K., and Mow, V.C. [1988]. A finite element formulation of the nonlinear biphasic model for articular cartilage and hydrated soft tissues including strain-dependent permeability. In R.L. Spilker and B.R. Simon, editors, *Computational Methods in Bioengineering*, pages 81–92. ASME.
- TNO Building and Construction Research [1993]. Parameter estimation. In *Diana 5.1 User's Manual*, volume 13. Delft, The Netherlands.
- Veldpaus, F.E., van de Molengraft, M.J.G., and Op den Camp, O.M.G.C. [1996]. Modeling and optimal estimation of mixtures –a simulation study–. accepted for publication in: *Inverse Problems in Engineering*.
- Yin, F.C.P., Chew, P.H., and Zeger, S.L. [1986]. An approach to quantification of biaxial tissue stress–strain data. *J. Biomech.*, 19(1), 27–37.

Appendix A

Finite element formulation of the model equations

The weighted residual method, combined with spatial discretisation, is used to transform the partial differential equations (2.15) and (2.20) into a set of ordinary first order differential equations and algebraic equations (Bathe [1982]).

Multiplication of the equations (2.15) and (2.20) by weighting functions g and \vec{h} and integration over the current mixture volume V results in

$$\int_V g \left(\vec{\nabla} \cdot \vec{q} - \vec{\nabla} \cdot (n^f(\vec{v}^f - \vec{v}^s)) \right) dV = 0, \quad (\text{A.1})$$

$$\int_V \vec{h} \cdot (\vec{\nabla} \cdot (\boldsymbol{\tau} - p\mathbf{I})) dV = 0. \quad (\text{A.2})$$

With Darcy's law (2.22) and Gauss' theorem this leads to

$$\int_V g \vec{\nabla} \cdot \vec{q} + \vec{\nabla} g \cdot \boldsymbol{\kappa} \cdot \vec{\nabla} p dV = \int_A g s dA, \quad (\text{A.3})$$

$$\int_V (\boldsymbol{\tau} - p\mathbf{I}) : (\vec{\nabla} \vec{h})^c dV = \int_A \vec{h} \cdot \vec{t} dA, \quad (\text{A.4})$$

where s is the fluid flow across the boundary, \vec{t} is the boundary stress vector, and $A = A(t)$ represents the current surface. Often it is advantageous to evaluate the integrand in the reference state. Then the integrals are transformed into integrals with respect to the reference configuration, resulting in

$$\int_{V_0} g (\mathbf{F}^{-c} \cdot \vec{\nabla}_0) \cdot \vec{q} + \vec{\nabla}_0 g \cdot \mathbf{F}^{-1} \cdot \boldsymbol{\kappa} \cdot \mathbf{F}^{-c} \cdot \vec{\nabla}_0 p J dV_0 = \int_{A_0} g s_0 J dA_0, \quad (\text{A.5})$$

$$\int_{V_0} (\boldsymbol{\tau} - p\mathbf{I}) : (\mathbf{F}^{-c} \cdot \vec{\nabla}_0 \vec{h})^c J dV_0 = \int_{A_0} \vec{h} \cdot \vec{t}_0 J dA_0, \quad (\text{A.6})$$

where

$$s_0 = n^f(\vec{v}^f - \vec{v}^s) \cdot (\mathbf{F}^{-c} \cdot \vec{n}_0), \quad (\text{A.7})$$

$$\vec{t}_0 = (\boldsymbol{\tau} - p\mathbf{I}) \cdot (\mathbf{F}^{-c} \cdot \vec{n}_0), \quad (\text{A.8})$$

and \vec{n}_0 is the unit outward normal on the reference surface. Equations (A.5) and (A.6) are discretised in space by means of the finite element method. The reference volume V_0 is subdivided in a finite number N_e of elements with a relatively simple shape (Bathe [1982]). In element e (volume V_0^e and surface A_0^e in the reference state), n_q displacement and n_p pressure nodes are introduced. The displacement vector of displacement node i of element e is denoted by \vec{q}_i^e , and the pressure in pressure node i of element e by p_i^e . Both \vec{q}_i^e and p_i^e are functions of time. Per element, columns \vec{q}^e and p^e are defined as

$$\vec{q}^e = [\vec{q}_1^e \cdots \vec{q}_{n_q}^e]^T, \quad p^e = [p_1^e \cdots p_{n_p}^e]^T. \quad (\text{A.9})$$

The displacement \vec{q} of a material point with position vector $\vec{x}_0 \in V_0^e$ is approximated by a linear combination of the displacements of the nodes of element e

$$\vec{q}(\vec{x}_0, t) = \underline{\psi}^T(\vec{x}_0) \vec{q}^e(t) \quad \forall \vec{x}_0 \in V_0^e, \quad (\text{A.10})$$

where $\underline{\psi}(\vec{x}_0) = [\psi_1(\vec{x}_0) \cdots \psi_{n_q}(\vec{x}_0)]^T$ is the column of displacement interpolation functions and ψ_i is the displacement interpolation function for nodal point i . This function satisfies $\psi_i(\vec{x}_{0j}) = \delta_{ij}$, where \vec{x}_{0j} is the reference position vector of nodal point j and δ_{ij} is the Kronecker function.

Similarly, the pressure in a material point $\vec{x}_0 \in V_0^e$ is approximated by a linear combination of the nodal pressures of element e

$$p(\vec{x}_0, t) = \underline{\phi}^T(\vec{x}_0) p^e(t) \quad \forall \vec{x}_0 \in V_0^e, \quad (\text{A.11})$$

where $\underline{\phi}(\vec{x}_0) = [\phi_1(\vec{x}_0) \cdots \phi_{n_p}(\vec{x}_0)]^T$ is the column of pressure interpolation functions such that $\phi_i(\vec{x}_{0j}) = \delta_{ij}$.

According to Galerkin's approximation method, the weighting functions \vec{h} and g are interpolated in the same way as the displacement, respectively the pressure, so

$$\vec{h}(\vec{x}_0, t) = \underline{\psi}^T(\vec{x}_0) \vec{h}^e(t) \quad \forall \vec{x}_0 \in V_0^e, \quad (\text{A.12})$$

$$g(\vec{x}_0, t) = \underline{\phi}^T(\vec{x}_0) g^e(t) \quad \forall \vec{x}_0 \in V_0^e. \quad (\text{A.13})$$

The gradients $\vec{\Psi}$ and $\vec{\Phi}$ of the interpolation functions are given by

$$\vec{\Psi}^T = \vec{\nabla}_0 \underline{\psi}^T, \quad \vec{\Phi}^T = \vec{\nabla}_0 \underline{\phi}^T. \quad (\text{A.14})$$

The deformation tensor \mathbf{F} follows from

$$\mathbf{F} = (\vec{\nabla}_0 \vec{x})^c = \mathbf{I} + (\vec{\nabla}_0 \vec{q})^c = \mathbf{I} + (\vec{q}^e)^T \vec{\Psi}, \quad (\text{A.15})$$

and with this result $J = \det(\mathbf{F})$, $\mathbf{C} = \mathbf{F}^c \cdot \mathbf{F}$ and $\vec{\nabla} = \mathbf{F}^{-c} \cdot \vec{\nabla}_0$ can be written as functions of \vec{q}^e . Elaboration of (A.5), using the fact that the integral over V_0 is equal to the sum of the integrals over the element volumes, yields

$$\sum_{e=1}^{N_e} (\underline{g}^e)^\tau \left[\underline{\vec{B}}^e \cdot \dot{\underline{q}}^e + \underline{K}^e \underline{p}^e - \underline{s}^e \right] = 0, \quad (\text{A.16})$$

where

$$\underline{\vec{B}}^e = \int_{V_0^e} \underline{\phi}(\mathbf{F}^{-c} \cdot \underline{\vec{\psi}}^\tau) J dV_0, \quad (\text{A.17})$$

$$\underline{K}^e = \int_{V_0^e} \underline{\vec{\Phi}} \cdot (\mathbf{F}^{-1} \cdot \underline{\kappa} \cdot \mathbf{F}^{-c}) \cdot \underline{\vec{\Phi}}^\tau J dV_0, \quad (\text{A.18})$$

$$\underline{s}^e = \int_{\bar{A}_0^e} \underline{\phi} s_0 J dA_0. \quad (\text{A.19})$$

Here, \bar{A}_0^e is the intersection of the boundary A_0^e of element e and the boundary A_0 of the mixture. Similarly, elaboration of (A.6) yields

$$\sum_{e=1}^{N_e} (\underline{h}^e)^\tau \cdot \left[\underline{\vec{f}}^e - (\underline{\vec{B}}^e)^\tau \underline{p}^e - \underline{\vec{t}}^e \right] = 0, \quad (\text{A.20})$$

where

$$\underline{\vec{f}}^e = \int_{V_0^e} (\underline{\vec{\psi}} \cdot \mathbf{F}^{-1} \cdot \underline{\tau}) J dV_0, \quad (\text{A.21})$$

$$\underline{\vec{t}}^e = \int_{\bar{A}_0^e} \underline{\psi} \underline{\vec{t}}_0 J dA_0. \quad (\text{A.22})$$

It is noted that $\underline{\vec{B}}^e$ does not depend on θ but, similarly to $\underline{\vec{f}}^e$ and \underline{K}^e , on \vec{q}^e . With $\underline{\tau}$ and $\underline{\kappa}$ according to (2.17) and (2.23) respectively, \underline{K}^e and $\underline{\vec{f}}^e$ can be written as

$$\underline{K}^e = \int_{V_0^e} \underline{\vec{\Phi}} \cdot \underline{\mathbf{K}} \cdot \underline{\vec{\Phi}}^\tau dV_0, \quad (\text{A.23})$$

$$\underline{\vec{f}}^e = \int_{V_0^e} \underline{\vec{\psi}} \cdot \underline{\mathbf{S}} \cdot \mathbf{F}^c dV_0. \quad (\text{A.24})$$

It is assumed that the second Piola-Kirchhoff stress tensor $\underline{\mathbf{S}}$ and the permeability tensor $\underline{\mathbf{K}}$ depend on the deformation tensor \mathbf{F} and on a set of local material parameters ϑ , i.e.

$$\underline{\mathbf{S}} = \underline{\mathbf{S}}(\mathbf{C}, \vartheta), \quad \underline{\mathbf{K}} = \underline{\mathbf{K}}(J, \vartheta), \quad (\text{A.25})$$

and that ϑ depends on the model parameters θ via

$$\vartheta = \underline{w}(\vec{x}_0, \theta). \quad (\text{A.26})$$

The terms in the equations (A.16) and (A.20) are functions of element quantities. To determine a set of equations in system quantities, an assembly process is required. Therefore, columns $\underline{\vec{q}}$, $\underline{\vec{p}}$, $\underline{\vec{h}}$, and \underline{g} are introduced

$$\underline{\vec{q}} = [\vec{q}_1 \dots \vec{q}_{N_q}]^T, \quad \underline{\vec{h}} = [\vec{h}_1 \dots \vec{h}_{N_q}]^T, \quad (\text{A.27})$$

$$\underline{\vec{p}} = [p_1 \dots p_{N_p}]^T, \quad \underline{g} = [g_1 \dots g_{N_p}]^T, \quad (\text{A.28})$$

where N_q and N_p are the number of system displacement and pressure nodes, respectively. Component i of these columns is equal to the corresponding quantity in system node i . Element quantities of element e are related to system quantities via the location matrices \underline{L}_q^e and \underline{L}_p^e , i.e.

$$\underline{\vec{q}}^e = \underline{L}_q^e \vec{q}, \quad \underline{\vec{h}}^e = \underline{L}_q^e \vec{h}, \quad (\text{A.29})$$

$$\underline{\vec{p}}^e = \underline{L}_p^e p, \quad \underline{g}^e = \underline{L}_p^e g. \quad (\text{A.30})$$

Substitution in (A.16) and (A.20), combined with the requirement that the equations have to hold for all \underline{g} and $\underline{\vec{h}}$, results in

$$\underline{\vec{B}} \cdot \underline{\vec{q}} + \underline{K} \underline{\vec{p}} - \underline{s} = \underline{0}, \quad (\text{A.31})$$

$$\underline{\vec{f}} - \underline{\vec{B}}^T \underline{\vec{p}} - \underline{\vec{t}} = \underline{\vec{0}}, \quad (\text{A.32})$$

where

$$\underline{\vec{B}} = \sum_{e=1}^{N_e} (\underline{L}_p^e)^T \underline{\vec{B}}^e (\underline{L}_q^e), \quad \underline{K} = \sum_{e=1}^{N_e} (\underline{L}_p^e)^T \underline{K}^e (\underline{L}_p^e), \quad (\text{A.33})$$

$$\underline{s} = \sum_{e=1}^{N_e} (\underline{L}_p^e)^T \underline{s}^e, \quad \underline{\vec{f}} = \sum_{e=1}^{N_e} (\underline{L}_q^e)^T \underline{\vec{f}}^e, \quad \underline{\vec{t}} = \sum_{e=1}^{N_e} (\underline{L}_q^e)^T \underline{\vec{t}}^e. \quad (\text{A.34})$$

An orthonormal vector base $\underline{\vec{e}} = [\vec{e}_1 \ \vec{e}_2 \ \vec{e}_3]^T$ with unit vectors \vec{e}_1 , \vec{e}_2 , and \vec{e}_3 is introduced. Then each nodal vector can be written as a linear combination of the base vectors, i.e.

$$\vec{q}_i = q_i^T \underline{\vec{e}}, \quad \vec{B}_{ij} = B_{ij}^T \underline{\vec{e}}, \quad \vec{f}_i = f_i^T \underline{\vec{e}}, \quad \vec{t}_i = t_i^T \underline{\vec{e}}. \quad (\text{A.35})$$

Here, q_i^T is the column with nodal displacements in the coordinate directions. The column with components of all nodal displacement vectors is equal to

$$\underline{q} = [q_1^T \dots q_{N_q}^T]^T. \quad (\text{A.36})$$

Similarly, $\underline{\vec{B}}$, $\underline{\vec{f}}$, and $\underline{\vec{t}}$ are composed of respectively B_{ij}^T , f_i^T , and t_i^T . In the coordinate system (A.31) and (A.32) become

$$\underline{\vec{B}} \underline{q} + \underline{K} \underline{\vec{p}} - \underline{s} = \underline{0}, \quad (\text{A.37})$$

$$\underline{\vec{f}} - \underline{\vec{B}}^T \underline{\vec{p}} - \underline{\vec{t}} = \underline{0}. \quad (\text{A.38})$$

To arrive at a set of equations in the unknown nodal quantities, the boundary conditions are accounted for. Part of the components of \underline{q} , \underline{p} , \underline{s} , and \underline{t} are known. If the displacement of a point at the surface of the material is prescribed in a certain direction, then in that point the force in that direction is not prescribed, and vice versa. In terms of the columns \underline{q} and \underline{t} , if q_i is prescribed then t_i is unknown, and if t_i is prescribed then q_i is unknown. Similar considerations hold for \underline{p} and \underline{s} . The columns \underline{q} and \underline{p} are subdivided in a part with known components (index k) and a part with unknown components (index l)

$$\underline{q}^r = [(\underline{q}^l)^r (\underline{q}^k)^r], \quad \underline{p}^r = [(\underline{p}^l)^r (\underline{p}^k)^r]. \quad (\text{A.39})$$

Here, \underline{q}^k and \underline{p}^k depend on the input \underline{u} , which contains all quantities that are set by the experimenter,

$$\underline{q}^k = \underline{q}^k(\underline{u}), \quad \underline{p}^k = \underline{p}^k(\underline{u}). \quad (\text{A.40})$$

The columns \underline{s} and \underline{t} are subdivided in, \underline{s}^l and \underline{t}^l corresponding to respectively unknown pressures and displacements, and \underline{s}^k and \underline{t}^k corresponding to prescribed pressures and displacements

$$\underline{s}^r = [(\underline{s}^l)^r (\underline{s}^k)^r], \quad \underline{t}^r = [(\underline{t}^l)^r (\underline{t}^k)^r]. \quad (\text{A.41})$$

Here, \underline{s}^l and \underline{t}^l depend on the input \underline{u} and on the displacements \underline{q}^l , but not on θ or on \underline{p}^l , so

$$\underline{s}^l = \underline{s}^l(\underline{q}^l, \underline{u}), \quad \underline{t}^l = \underline{t}^l(\underline{q}^l, \underline{u}). \quad (\text{A.42})$$

Dependency on \underline{q}^l results from the fact that \underline{s}^l and \underline{t}^l are determined by integration over the current surface \bar{A}_0^e of the elements, which depends on the deformation. Partitioning and rearranging results in a set of equations, from which \underline{q}^l and \underline{p}^l can be solved

$$\underline{B}^{ll} \underline{q}^l + \underline{K}^{ll} \underline{p}^l - \underline{s}^l + \underline{B}^{lk} \underline{q}^k + \underline{K}^{lk} \underline{p}^k = \underline{0}, \quad (\text{A.43})$$

$$\underline{f}^l - (\underline{B}^{ll})^r \underline{p}^l - \underline{t}^l - (\underline{B}^{kl})^r \underline{p}^k = \underline{0}, \quad (\text{A.44})$$

with initial condition $\underline{q}^l(t_0) = \underline{q}_0^l$. When \underline{q}^l , \underline{q}^k , and \underline{p}^l are computed, \underline{s}^k and \underline{t}^k can be determined using

$$\underline{s}^k = \underline{B}^{kl} \underline{q}^l + \underline{B}^{kk} \underline{q}^k + \underline{K}^{kl} \underline{p}^l + \underline{K}^{kk} \underline{p}^k, \quad (\text{A.45})$$

$$\underline{t}^k = \underline{f}^k - (\underline{B}^{lk})^r \underline{p}^l - (\underline{B}^{kk})^r \underline{p}^k. \quad (\text{A.46})$$

The distinct terms in (A.43), (A.44), (A.45), and (A.46) are known smooth functions of their arguments according to

$$\underline{B} = \underline{B}(\underline{q}^l, \underline{u}), \quad \underline{K} = \underline{K}(\underline{q}^l, \theta, \underline{u}), \quad \underline{f} = \underline{f}(\underline{q}^l, \theta, \underline{u}). \quad (\text{A.47})$$

The components of \underline{f} and \underline{K} depend on $\underline{\theta}$ since τ and κ are functions of the model parameters. Furthermore, \underline{K}^u is symmetric and semi-positive definite

$$\underline{K}^u = (\underline{K}^u)^\tau, \quad \underline{K}^u \geq \underline{0}. \quad (\text{A.48})$$

As an abbreviation, two columns are introduced

$$\underline{s}^* = \underline{s}^l - \underline{B}^{lk} \underline{q}^k - \underline{K}^{lk} \underline{p}^k = \underline{s}^*(\underline{q}^l, \underline{\theta}, \underline{u}, \underline{\dot{u}}), \quad (\text{A.49})$$

$$\underline{t}^* = \underline{t}^l + (\underline{B}^{kl})^\tau \underline{p}^k = \underline{t}^*(\underline{q}^l, \underline{u}). \quad (\text{A.50})$$

For clarity, the indices l , k , and $*$, will be omitted in the remainder of this thesis. Then, the describing set of equations becomes

$$\underline{B} \underline{\dot{q}} + \underline{K} \underline{p} = \underline{s}, \quad (\text{A.51})$$

$$\underline{f} - \underline{B}^\tau \underline{p} = \underline{t}. \quad (\text{A.52})$$

A number of auxiliary quantities are introduced. The components of \underline{f} , \underline{s} , and \underline{t} are smooth functions of their arguments. Therefore, the variations $\delta \underline{f}$, $\delta \underline{s}$, and $\delta \underline{t}$ of respectively \underline{f} , \underline{s} , and \underline{t} as a result of variations of \underline{q} and $\underline{\theta}$ can be written as

$$\delta \underline{f} = \underline{F}^q \delta \underline{q} + \underline{F}^\theta \delta \underline{\theta}, \quad (\text{A.53})$$

$$\delta \underline{s} = \underline{S}^q \delta \underline{q} + \underline{S}^\theta \delta \underline{\theta}, \quad (\text{A.54})$$

$$\delta \underline{t} = \underline{T}^q \delta \underline{q} + \underline{T}^\theta \delta \underline{\theta}, \quad (\text{A.55})$$

where

$$(\underline{F}^\alpha)_{ij} = \frac{\partial f_i}{\partial \alpha_j}, \quad \underline{F}^\alpha = \underline{F}^\alpha(\underline{q}, \underline{\theta}, \underline{u}), \quad (\text{A.56})$$

$$(\underline{S}^\alpha)_{ij} = \frac{\partial s_i}{\partial \alpha_j}, \quad \underline{S}^\alpha = \underline{S}^\alpha(\underline{q}, \underline{\theta}, \underline{u}, \underline{\dot{u}}), \quad (\text{A.57})$$

$$(\underline{T}^\alpha)_{ij} = \frac{\partial t_i}{\partial \alpha_j}, \quad \underline{T}^\alpha = \underline{T}^\alpha(\underline{q}, \underline{u}), \quad (\text{A.58})$$

for $\alpha \in \{q, \theta\}$. As \underline{t} does not depend on the model parameters, $\underline{T}^\theta = \underline{0}$. Variations of \underline{u} and $\underline{\dot{u}}$ do not occur, since \underline{u} is known at every time point t . Also variations $\delta \underline{B}$ and $\delta \underline{K}$ of respectively \underline{B} and \underline{K} are of interest. To avoid the use of three-dimensional matrices, only variations of the matrix multiplications $\underline{B} \underline{a}$ and $\underline{K} \underline{b}$ are considered, where \underline{a} and \underline{b} contain the same number of components as respectively \underline{q} and \underline{p}

$$\underline{B}(\underline{q} + \delta \underline{q}, \underline{u}) \underline{a} = \underline{B}(\underline{q}, \underline{u}) \underline{a} + \underline{D}^q(\underline{q}, \underline{a}, \underline{u}) \delta \underline{q}, \quad (\text{A.59})$$

$$\underline{K}(\underline{q} + \delta \underline{q}, \underline{\theta}, \underline{u}) \underline{b} = \underline{K}(\underline{q}, \underline{\theta}, \underline{u}) \underline{b} + \underline{M}^q(\underline{q}, \underline{b}, \underline{\theta}, \underline{u}) \delta \underline{q}, \quad (\text{A.60})$$

$$\underline{K}(\underline{q}, \underline{\theta} + \delta \underline{\theta}, \underline{u}) \underline{b} = \underline{K}(\underline{q}, \underline{\theta}, \underline{u}) \underline{b} + \underline{M}^\theta(\underline{q}, \underline{b}, \underline{\theta}, \underline{u}) \delta \underline{\theta}, \quad (\text{A.61})$$

with

$$(\underline{D}^q)_{ij} = \sum_k \frac{\partial B_{ik}}{\partial q_j} a_k, \quad (\underline{M}^q)_{ij} = \sum_k \frac{\partial K_{ik}}{\partial q_j} b_k, \quad (\underline{M}^\theta)_{ij} = \sum_k \frac{\partial K_{ik}}{\partial \theta_j} b_k. \quad (\text{A.62})$$

Let $\delta \underline{q}$ and $\delta \underline{p}$ be variations on \underline{q} , respectively \underline{p} as a result of a variation $\delta \underline{\theta}$ on the model parameters. The varied solutions $\underline{q} + \delta \underline{q}$ and $\underline{p} + \delta \underline{p}$ still have to satisfy the model equations (A.51) and (A.52). To derive the relation between $\delta \underline{q}$, $\delta \underline{p}$ and $\delta \underline{\theta}$, the varied solutions are substituted in (A.51) and (A.52) and subsequently linearised by applying a Taylor's series expansion around \underline{q} , \underline{p} and $\underline{\theta}$, neglecting all terms of second or higher order in $\delta \underline{q}$, $\delta \underline{p}$, and $\delta \underline{\theta}$. This results in

$$\underline{B} \delta \dot{\underline{q}} + \underline{L}^{sq} \delta \underline{q} + \underline{L}^{sp} \delta \underline{p} + \underline{L}^{s\theta} \delta \underline{\theta} = 0, \quad (\text{A.63})$$

$$\underline{L}^{tq} \delta \underline{q} + \underline{L}^{tp} \delta \underline{p} + \underline{L}^{t\theta} \delta \underline{\theta} = 0, \quad (\text{A.64})$$

where

$$\underline{L}^{sq} = \underline{D}^q(\underline{q}, \dot{\underline{q}}, \underline{u}) + \underline{M}^q(\underline{q}, \underline{p}, \underline{\theta}, \underline{u}) - \underline{S}^q(\underline{q}, \underline{\theta}, \underline{u}, \dot{\underline{u}}), \quad (\text{A.65})$$

$$\underline{L}^{tq} = \underline{F}^q(\underline{q}, \underline{\theta}, \underline{u}) - \left(\underline{D}^q(\underline{q}, \underline{p}, \underline{u}) \right)^T - \underline{T}^q(\underline{q}, \underline{u}), \quad (\text{A.66})$$

$$\underline{L}^{sp} = \underline{K}(\underline{q}, \underline{\theta}, \underline{u}), \quad (\text{A.67})$$

$$\underline{L}^{tp} = - \left(\underline{B}(\underline{q}, \underline{\theta}) \right)^T, \quad (\text{A.68})$$

$$\underline{L}^{s\theta} = \underline{M}^\theta(\underline{q}, \underline{p}, \underline{\theta}, \underline{u}) - \underline{S}^\theta(\underline{q}, \underline{\theta}, \underline{u}, \dot{\underline{u}}), \quad (\text{A.69})$$

$$\underline{L}^{t\theta} = \underline{F}^\theta(\underline{q}, \underline{\theta}, \underline{u}). \quad (\text{A.70})$$

The determination of $\underline{L}^{s\theta}$ and $\underline{L}^{t\theta}$, which are required for parameter estimation, is not part of the standard protocol in finite element analyses. Therefore, the determination of \underline{M}^θ will be discussed as an example. Likewise \underline{S}^θ and \underline{F}^θ are set up.

Since \underline{K} is equal to the assembly of the element matrices \underline{K}^e , the term $\underline{K} \underline{p}$ can be written as

$$\underline{K} \underline{p} = \left(\sum_{e=1}^{N_e} (\underline{L}_p^e)^T \underline{K}^e (\underline{L}_p^e) \right) \underline{p}, \quad \underline{K}^e = \int_{V_0^e} \vec{\Phi} \cdot \underline{K} \cdot \vec{\Phi}^T dV_0, \quad (\text{A.71})$$

using (A.33) and (A.23). Since V_0^e , \underline{L}_p^e , $\vec{\Phi}$ and \underline{p} do not explicitly depend on $\underline{\theta}$, the derivative of $\underline{K} \underline{p}$ to component k of $\underline{\theta}$ is equal to

$$(\underline{M}^\theta)_k = \left(\sum_{e=1}^{N_e} (\underline{L}_p^e)^T \frac{\partial \underline{K}^e}{\partial \theta_k} (\underline{L}_p^e) \right) \underline{p}, \quad \frac{\partial \underline{K}^e}{\partial \theta_k} = \int_{V_0^e} \vec{\Phi} \cdot \frac{\partial \underline{K}}{\partial \theta_k} \cdot \vec{\Phi}^T dV_0, \quad (\text{A.72})$$

where $(\underline{M}^\theta)_k$ denotes column k of \underline{M}^θ . The derivative of the tensor function \underline{K} to the model parameters can be determined analytically according to

$$\frac{\partial \underline{K}}{\partial \theta_k} = \sum_{l=1}^{n_\theta} \frac{\partial \underline{K}}{\partial \vartheta_l} \frac{\partial \vartheta_l}{\partial \theta_k}, \quad (\text{A.73})$$

where (2.24) is used. Herein, n_ϑ is the number of local material parameters in ϑ . Equation (A.72) shows that $(\underline{M}^\vartheta)_k$ can be assembled from the element contributions $\partial \mathbf{K} / \partial \theta_k$ in the same way as \underline{K} from \mathbf{K} . This procedure is repeated for $k \in \{1, \dots, N_\vartheta\}$, where N_ϑ is the number of model parameter in ϑ .

Appendix B

Scheme of the recursive algorithm

- I. Start computations
Set measurement counter $r = 0$
- II. Elaboration of measurement $r + 1$
Set initial conditions $\hat{\underline{\theta}}_r, \underline{q}_r$
Input measurement \underline{m}_{r+1}
Set parameter iteration counter $l = 1$
Approximate $\hat{\underline{\theta}}_{r+1}^{(l)}$ as the previous estimate $\hat{\underline{\theta}}_r$
- III. Solve estimation problem
Set time step counter $j = 1$
- IV. Execute time step $\Delta t = \frac{1}{k}(t_{r+1} - t_r)$; $t_{r,j} = t_r + j\Delta t$
Set iteration counter $m = 1$
Approximate $\hat{\underline{q}}_{r,j}^{(m)}$ as $\hat{\underline{q}}_{r,j-1}$ and $\hat{\underline{p}}_{r,j}^{(m)}$ as $\hat{\underline{p}}_{r,j-1}$
- V. Solve model equations
Determine $\Delta \underline{q}$ and $\Delta \underline{p}$ from (2.44) and (2.45)
Update: $\underline{q}_{r,j}^{(m+1)} = \underline{q}_{r,j}^{(m)} + \Delta \underline{q}$ and $\underline{p}_{r,j}^{(m+1)} = \underline{p}_{r,j}^{(m)} + \Delta \underline{p}$
If $\{ \Delta \underline{q} \text{ and } \Delta \underline{p} \text{ not sufficiently small} \}$ then $\{ m := m + 1, \text{ go to V} \}$
Determine $\underline{Q}_{r,j}$ and $\underline{P}_{r,j}$ from (2.58) and (2.59)
If $\{ j < k \}$ then $\{ j := j + 1, \text{ go to IV} \}$
Determine \underline{y}_{r+1} from (2.61) and \underline{H}_{r+1} from (2.63)
Determine $\Delta \underline{\theta}$ from (3.10)
Update: $\hat{\underline{\theta}}_{r+1}^{(l+1)} = \hat{\underline{\theta}}_{r+1}^{(l)} + \Delta \underline{\theta}$
If $\{ \Delta \underline{\theta} \text{ not sufficiently small} \}$ then $\{ l := l + 1, \text{ go to III} \}$
If $\{ r < N - 1 \}$ then $\{ r := r + 1, \text{ go to II} \}$
- VI. Stop computations

Appendix C

Formulation of the boundary value problem

In Chapter 4, an identification model, consisting of model equations, a parameter equation and a measurement equation, is introduced. Objective of the identification procedure is to find solutions $\hat{\theta}(\tau)$, $\hat{q}(\tau)$ and $\hat{p}(\tau)$ for $\tau \in [t_0, t_N]$ which minimise the residuals on the identification model. For this purpose, an augmented scalar measure J^* (4.6) of the residuals is introduced. The requirement that J^* is minimal results in a boundary value problem.

The augmented measure J^* depends on $\theta(\tau)$, $q(\tau)$, $p(\tau)$, $\xi_1(\tau)$, $\xi_3(\tau)$, $\lambda(\tau)$, $\mu(\tau)$ and $u(\tau) \mid \tau \in [t_0, t_N]$ and is given by

$$J^* = \int_{t_0}^{t_N} \left\{ \frac{1}{2}(\underline{f} - \underline{B}^T \underline{p} - \underline{t})^T \underline{W}_2 (\underline{f} - \underline{B}^T \underline{p} - \underline{t}) + \frac{1}{2}(\underline{m} - \underline{g})^T \underline{V} (\underline{m} - \underline{g}) + \right. \quad (C.1)$$

$$\left. \frac{1}{2} \underline{\xi}_1^T \underline{W}_1 \underline{\xi}_1 + \frac{1}{2} \underline{\xi}_3^T \underline{W}_3 \underline{\xi}_3 + \lambda^T [\underline{B} \underline{q} + \underline{K} \underline{p} - \underline{s} - \underline{\xi}_1] + \mu^T [\underline{\theta} - \underline{\xi}_3] \right\} d\tau,$$

where the accent circumflex on θ , q , and p is omitted for clarity. A necessary condition for J^* to be minimal is that the variation δJ^* of J^* equals 0. Using (A.53) to (A.55), (A.59) to (A.61), and (2.62), the variation δJ^* as a result of variation of θ , q , p , ξ_1 , ξ_3 , λ and μ is given by

$$\delta J^* = \int_{t_0}^{t_N} \left\{ \delta \theta^T [(\underline{F}^\theta)^T \underline{W}_2 (\underline{f} - \underline{B}^T \underline{p} - \underline{t}) + (\underline{M}^\theta - \underline{S}^\theta)^T \underline{\lambda}] + \delta \theta^T [\underline{\mu}] + \right. \quad (C.2)$$

$$\delta q^T [(\underline{F}^q - (\underline{D}^q)^T - \underline{T}^q)^T \underline{W}_2 (\underline{f} - \underline{B}^T \underline{p} - \underline{t}) - (\underline{G}^q)^T \underline{V} (\underline{m} - \underline{g}) + (\underline{D}^q + \underline{M}^q - \underline{S}^q)^T \underline{\lambda}] +$$

$$\delta p^T [\underline{B}^T \underline{\lambda}] + \delta p^T [-\underline{B} \underline{W}_2 (\underline{f} - \underline{B}^T \underline{p} - \underline{t}) - (\underline{G}^p)^T \underline{V} (\underline{m} - \underline{g}) + \underline{K}^T \underline{\lambda}] +$$

$$\delta \xi_1^T [\underline{W}_1 \underline{\xi}_1 - \underline{\lambda}] + \delta \xi_3^T [\underline{W}_3 \underline{\xi}_3 - \underline{\mu}] + \delta \lambda^T [\underline{B} \underline{q} + \underline{K} \underline{p} - \underline{s} - \underline{\xi}_1] + \delta \mu^T [\underline{\theta} - \underline{\xi}_3] \left. \right\} d\tau,$$

where all terms of second or higher order in the variations are neglected. Since the input is known, no variations of u occur. The terms with $\delta \theta$ and δq are partially integrated, i.e.

$$\int_{t_0}^{t_N} \delta \theta^T [\underline{\mu}] d\tau = \delta \theta^T(t_N) [\underline{\mu}(t_N)] - \delta \theta^T(t_0) [\underline{\mu}(t_0)] - \int_{t_0}^{t_N} \delta \theta^T [\dot{\underline{\mu}}] d\tau, \quad (C.3)$$

$$\int_{t_0}^{t_N} \delta \dot{q}^T [\underline{B}^T \lambda] d\tau = \delta q^T(t_N) [\underline{B}^T \lambda(t_N)] - \delta q^T(t_0) [\underline{B}^T \lambda(t_0)] - \int_{t_0}^{t_N} \delta q^T [\dot{\underline{B}}^T \lambda + \underline{B}^T \dot{\lambda}] d\tau. \quad (C.4)$$

The requirement $\delta J^* = 0$ for all $\delta \theta$, δq , δp , $\delta \xi_1$, $\delta \xi_3$, $\delta \lambda$ and $\delta \mu$ leads to

$$(\underline{L}^{t\theta})^T \underline{W}_2 (\underline{f} - \underline{B}^T \underline{p} - \underline{t}) + (\underline{L}^{s\theta})^T \lambda - \dot{\mu} = \underline{0}, \quad (C.5)$$

$$\underline{\mu}(t_0) = \underline{0}, \quad \underline{\mu}(t_N) = \underline{0}, \quad (C.6)$$

$$(\underline{L}^{tq})^T \underline{W}_2 (\underline{f} - \underline{B}^T \underline{p} - \underline{t}) - (\underline{G}^q)^T \underline{V} (\underline{m} - \underline{g}) + (\underline{L}^{sq})^T \lambda - (\dot{\underline{B}}^T \lambda + \underline{B}^T \dot{\lambda}) = \underline{0}, \quad (C.7)$$

$$\underline{B}^T \lambda(t_0) = \underline{0}, \quad \underline{B}^T \lambda(t_N) = \underline{0}, \quad (C.8)$$

$$-\underline{B} \underline{W}_2 (\underline{f} - \underline{B}^T \underline{p} - \underline{t}) - (\underline{G}^p)^T \underline{V} (\underline{m} - \underline{g}) + \underline{K}^T \lambda = \underline{0}, \quad (C.9)$$

$$\underline{W}_1 \xi_1 - \lambda = \underline{0}, \quad (C.10)$$

$$\underline{W}_3 \xi_3 - \mu = \underline{0}, \quad (C.11)$$

$$\underline{B} \dot{q} + \underline{K} \underline{p} - \underline{s} - \xi_1 = \underline{0}, \quad (C.12)$$

$$\dot{\theta} - \xi_3 = \underline{0}, \quad (C.13)$$

where (A.65) to (A.70) are used. These equations can be reordered to yield (4.7) to (4.15).

Appendix D

The transformation matrix in the approximating linearisation method

Substitution of (4.28) and (4.29) in (4.25) and (4.26) followed by linearisation of \underline{z} and \underline{g} around $\underline{\omega}$ results in

$$\dot{\underline{\omega}} + \underline{\Omega} \dot{\underline{\lambda}} + \underline{\Omega} \dot{\underline{\lambda}} = \underline{z}(\underline{\omega}, \underline{y}) + \underline{Z} \underline{\Omega} \dot{\underline{\lambda}} + \underline{W}^{-1} \dot{\underline{\lambda}}, \quad (\text{D.1})$$

$$\dot{\underline{\lambda}} = -\underline{Z}^T \dot{\underline{\lambda}} - \underline{G}^T \underline{V} (\underline{m} - \underline{g}(\underline{\omega}, \underline{y})) + \underline{G}^T \underline{V} \underline{G} \underline{\Omega} \dot{\underline{\lambda}}. \quad (\text{D.2})$$

Substitution of $\dot{\underline{\lambda}}$ according to (D.2) in (D.1) yields after reordering

$$\begin{aligned} \dot{\underline{\omega}} &= \underline{z}(\underline{\omega}, \underline{y}) + \underline{\Omega} \underline{G}^T \underline{V} (\underline{m} - \underline{g}(\underline{\omega}, \underline{y})) + \\ &- \left[\underline{\Omega} - \underline{W}^{-1} - \underline{\Omega} \underline{Z}^T - \underline{Z} \underline{\Omega} + \underline{\Omega} \underline{G}^T \underline{V} \underline{G} \underline{\Omega} \right] \dot{\underline{\lambda}}. \end{aligned} \quad (\text{D.3})$$

If $\underline{\Omega}$ satisfies

$$\underline{\Omega} = \underline{W}^{-1} + \underline{\Omega} \underline{Z}^T + \underline{Z} \underline{\Omega} - \underline{\Omega} \underline{G}^T \underline{V} \underline{G} \underline{\Omega}, \quad (\text{D.4})$$

the term between brackets in (D.3) is equal to \underline{Q} and a nonlinear differential equation in $\underline{\omega}$ results.

Curriculum Vitae

Olaf Op den Camp werd op 1 oktober 1968 geboren te Swalmen. Hij volgde van 1980 tot 1986 het Gymnasium- β op het Bisschoppelijk College Broekhin in Roermond. In 1986 begon hij met de studie Werktuigbouwkunde aan de Technische Universiteit Eindhoven. Daarnaast startte hij in 1988 met de studierichting Werktuigkundig Medische Technologie. Beide studierichtingen werden in 1991 afgerond met een afstudeeronderzoek naar een theoretisch model van de smeerfilm in het menselijk kniegewricht. Van 1991 tot 1995 verrichtte hij een promotieonderzoek bij de vakgroep Fundamentele Werktuigkunde van de Technische Universiteit Eindhoven, waarvan dit proefschrift het resultaat is. Sinds oktober 1995 is hij als wetenschappelijk medewerker verbonden aan de afdeling glastechnologie van TNO-Technisch Fysische Dienst in Eindhoven.

Dankwoord

Graag wil ik iedereen die op zijn of haar manier heeft bijgedragen aan de totstandkoming van dit proefschrift van harte bedanken:

- collega's, medewerkers en studenten van de vakgroep Fundamentele Werktuigkunde van de Technische Universiteit Eindhoven,
- mijn kamergenoten Peter, Patricia en Carlijn,
- medewerkers van de afdeling Numerieke Mechanica van TNO-Bouw te Rijswijk, met name Max Hendriks,
- ouders, vrienden en natuurlijk Ilona.

Olaf Op den Camp,
Deurne, 8 mei 1996.

Samenvatting

Standaardmethoden voor het bepalen van materiaalparameters gaan meestal uit van zodanige proefstukvormen en belastingen dat gemeten randbelastingen en -verplaatsingen eenvoudig om te rekenen zijn naar lokale spanningen en rekken, waaruit vervolgens de parameters in een aangenomen materiaalmodel kunnen worden bepaald. Voor veel (complexe) materialen zijn deze methoden lastig of niet te gebruiken, bijvoorbeeld omdat het materiaal inhomogeen is of omdat het maken van proefstukken lastig of ongewenst is. In dergelijke situaties kan de numeriek-experimentele methode bruikbaar zijn. Daarbij wordt naast randinformatie gebruik gemaakt van gemeten veldinformatie (verplaatsingsvelden, drukken, snelheden). Door deze informatie te confronteren met (numerieke) berekeningen op basis van een verondersteld materiaalmodel en beginschattingen voor onbekende materiaalparameters kunnen via een schattingsalgoritme parameters iteratief worden aangepast tot convergentie wordt bereikt. Deze methode biedt veel meer vrijheid dan standaard experimentele methoden, maar is tot nu toe vooral toegepast op materialen die tijdsafhankelijk gedrag vertonen.

De doelstelling van dit proefschrift was om enkele algoritmen te onderzoeken die bruikbaar zijn voor materialen die tijdsafhankelijk gedrag vertonen. Een volledig recursief en een integraal schattingsalgoritme zijn geïmplementeerd en onderzocht. Ze zijn toegepast op mengselmaterialen, bestaande uit een poreuze vaste stof, verzadigd met vloeistof. De interactie tussen vaste stof en vloeistof leidt tot visco-elastisch gedrag.

De differentiaal- en algebraïsche modelvergelijkingen die het gedrag beschrijven zijn niet-lineair in de verplaatsingen en materiaalparameters en lineair in de drukken. De gebruikte veldinformatie bestaat uit drukken en verplaatsingen. De algoritmen zijn getest door middel van simulaties. De resultaten van een analyse met een gekozen materiaalmodel en gekozen materiaalparameters, representeren na verstoring met ruis, observaties uit een experiment. Het schattingsmodel wordt vervolgens gestart met gewijzigde waarden voor de parameters. Het verschil tussen de 'experimentele' resultaten en de resultaten van analyses met het model wordt gebruikt om de gekozen parameters terug te schatten met het schattingsalgoritme. Er zijn analyses uitgevoerd met en zonder modelfouten.

De belangrijkste conclusie is dat beide algoritmen in principe bruikbaar zijn om materiaalparameters te bepalen voor dit type materialen. Het recursieve algoritme is bijzonder efficiënt. De tijd die nodig is om materiaalparameters te schatten is van dezelfde orde van grootte als de tijd die nodig is voor één enkele analyse met gegeven parameters. Het integraal algoritme is nog erg tijdrovend en leidt tot een lastig twee-punts-randwaarde probleem, waar op dit moment nog geen algemeen toepasbare, bevredigende oplosstrategie voor gevonden is.

Stellingen

behorende bij het proefschrift

Identification Algorithms for Time-Dependent Materials

1. Het recursieve schattingsalgoritme maakt de praktische toepassing van de numeriek-experimentele methode voor materialen die tijdsafhankelijk gedrag vertonen mogelijk.

Dit proefschrift: hoofdstuk 3

2. Wanneer het integraal schattingsalgoritme gebruikt wordt om de modelparameters van een vloeistof-vaste stof mengsel te bepalen, ontstaat een twee-punts-randwaarde probleem dat op dit moment slechts bij uitzondering is op te lossen.

Dit proefschrift: hoofdstuk 4

3. Identificatie is succesvol als het verschil tussen de metingen en de op basis van een verondersteld materiaalmodel berekende waarden voor de gemeten grootheden na schatten van de parameters te verklaren is.

4. Tijdens het recursief schatten moet duidelijk onderscheid worden gemaakt tussen schattingen voor de parameters bij achtereenvolgende iteraties op basis van metingen op een zeker tijdstip en schattingen op basis van metingen op achtereenvolgende tijdstippen. Opeenvolgende iteratieve waarden geven enkel inzicht in hoeverre aan de niet-lineaire vergelijking voor de parameters wordt voldaan. Waarden voor de parameters op achtereenvolgende tijdstippen kunnen informatie geven over het hele identificatieprobleem.

Dit proefschrift: hoofdstuk 3

5. De mate waarin het schattingsproces is geconvergeerd kan niet zonder meer worden afgelezen aan het verschil tussen de parameters die bepaald zijn aan de hand van opeenvolgende metingen. Dit verschil is mogelijk klein door een geringe gevoeligheid van de uitgang met betrekking tot de parameters. Derhalve moet zowel tijdens het ontwerp van een experiment als tijdens het schatten zelf de gevoeligheid bestudeerd worden.

6. De ontwikkeling van snellere hardware moet hand in hand gaan met de ontwikkeling van efficiëntere software om de gebruiker echt tevreden te kunnen stellen.

7. Ofschoon glas een eeuwenoud produkt is, zal het ook in de toekomst onderwerp van onderzoek blijven aangezien de eisen met betrekking tot het produkt en de produktie sterk toenemen.
8. Ondanks uitgebreid onderzoek is er weinig bekend over de diffusie van gassen in een glas-smelt.
Krämer, F. [1979]. Mathematisches Modell der Veränderung von Gasblasen in Glas-schmelzen. Glastechnische Berichte 52(2), 43–50.
9. De geschiedenis leert ons dat de toekomst anders zal zijn dan we nu denken.
10. Muziek moet je maken met je hart en je hart kun je maken met muziek.

Olaf Op den Camp
Eindhoven, 8 mei 1996

For many 'complex' materials it is impossible to determine the material parameters with standard methods. In these situations numerical-experimental techniques offer much more possibilities. By confronting measured quantities, such as displacements and pressures, with calculations on the basis of an assumed material model via an identification algorithm, the material parameters are determined.

In this thesis, algorithms suitable for materials showing time-dependent behaviour have been studied. These algorithms have to determine all parameters on the basis of quantities that are measured not only at different positions within the material (*space*) but also at subsequent points of *time*. A fully recursive and an integral algorithm have been tested on a mixture of a solid and a fluid. Both algorithms appeared to be applicable to this type of time-dependent material. Moreover, it is expected that the algorithms can be applied to other visco-elastic materials without many problems.